Timing mechanism of sexually dimorphic nervous system differentiation

Laura Pereira[1], Florian Aeschimann[2], Chen Wang[1], Hannah Lawson[3], Esther Serrano-Saiz[1], Douglas S. Portman[3], Helge Großhans[2] and Oliver Hobert[1]

[1] Department of Biological Sciences, Howard Hughes Medical Institute, Columbia University, New York, NY, USA

[2] Friedrich Miescher Institute for Biomedical Research, Basel, Switzerland

[3] DelMonte Institute for Neuroscience, Departments of Biomedical Genetics, Neuroscience, and Biology, University of Rochester, Rochester, New York, USA

ABSTRACT

In all animals, sexual differentiation of somatic tissue is precisely timed, yet the molecular mechanisms that control the timing of sexual differentiation, particularly in the brain, are poorly understood. We have used several sexually dimorphic molecular, anatomical and behavioral features of the *C. elegans* nervous system to decipher a regulatory pathway that controls the precise timing of sexual differentiation. We find that the sexually dimorphic differentiation of embryonically born, sex-shared neurons is independent of the gonad, but is tightly coupled to the heterochronic pathway that was shown to control the timing of epidermal cell lineage division patterns. Sexually dimorphic differentiation of postmitotic neurons in the male nervous system is abrogated in animals that carry a mutation in the heterochronic miRNA *let-7* and prematurely executed in animals either lacking the *let-7* inhibitor *lin-28,* or the direct *let-7* target *lin-41*, an RNA-binding, posttranscriptional regulator. We show that an isoform of a phylogenetically conserved Zn finger transcription factor, *lin-29a,* is a critical target of LIN-41 in controlling sexual maturation of sex-shared neurons. Temporally controlled *lin-29a* is expressed in a male-specific manner in a subset of sex-shared neurons. *lin-29a* acts cell-autonomously in these neurons to control the expression of sexually dimorphic neurotransmitter switches, sensory receptor expression, neurite anatomy and connectivity, and locomotor behavior. *lin-29a* is not only required but also sufficient to impose male-specific features at earlier stages of development and in the opposite sex. The temporal, sexual and spatial specificity of *lin-29a* expression is controlled intersectionally through the heterochronic pathway, sex chromosome configuration and neuron type-specific terminal selector transcription factors. Two Doublesex-like transcription factors represent additional neuron-type specific targets of LIN-41 and are regulated in a similar intersectional manner, indicating the existence of modular outputs downstream of the heterochronic pathway. In conclusion, we have provided insights into the molecular logic of the timing of sexual differentiation in the *C. elegans* nervous system. Remarkably, the *lin28/let7* axis also controls the timing of sexual differentiation in mice and humans thereby hinting toward a striking universality of the control mechanisms of sexual differentiation.

INTRODUCTION

Throughout the animal kingdom, the brains of males and females display anatomical and functional differences (Jazin and Cahill, 2010; McCarthy and Arnold, 2011). Most neuronal dimorphisms arise during sexual maturation and these maturation events are timed to occur during specific windows of postnatal life. For example, in mammals, puberty is a key developmental transition that defines the boundary between immaturity from adulthood and is accompanied by substantial sexually dimorphic changes in the brain (Avendano et al., 2017; Juraska and Willing, 2017; Sisk and Foster, 2004). However, despite the realization that sexual maturation occurs during specific periods of development, little is known about the timing mechanism of sexually dimorphic maturation in the brain.

Specific neuronal populations in the mammalian brain control the onset of sexual maturation via the use of several hormonal systems, including gonadotropin-releasing hormone (GnRH) and kisspeptin (Avendano et al., 2017). The onset of puberty is driven by the enhancement in the neurosecretory activity of GnRH neurons, and several neuronal populations have been shown to regulate the activity of GnRH neurons. However, how these neuronal activation mechanisms are timed to occur at a specific developmental window is not known. Recent studies have provided tantalizing hints toward potential timing mechanisms (Faunes and Larrain, 2016). Specifically, loss and gain of function studies of the miRNA Let7 and Lin28, a protein involved in *let-7* miRNA processing, have shown that these factors can affect the timing of puberty in mice (Corre et al., 2016; Zhu et al., 2010). Moreover, genetic association studies have linked Lin28 to the timing of puberty in humans (Chen et al., 2017; He et al., 2009; Ong et al., 2009; Perry et al., 2009; Sulem et al., 2009). The expression of Lin28 and Let7 in the hypothalamus, a site of release of peptides that control pubertal onset, is temporally controlled (Sangiao-Alvarellos et al., 2013), but the cellular and molecular mechanisms of Lin28/Let7 have not been deciphered in the context of controlling the timing of sexual maturation in the mammalian brain.

What is remarkable about the involvement of the miRNA Let7 and its processing regulator Lin28 in puberty control in mice and humans is that these two genes are well-established developmental timers of non-neuronal tissue types in the nematode *C. elegans* (Moss et al., 1997; Reinhart et al., 2000). In this paper, we provide evidence for a potential universality of the Lin28/Let7 axis in controlling the onset of sexual maturation in the nervous system. We show here that these genes control the timing of sexual dimorphic nervous system differentiation in *C. elegans* and identify phylogenetically conserved, functionally relevant targets of these factors.

Like in many other animal species, sexual maturation of somatic tissue of the nematode *C. elegans* is precisely timed to occur at specific stages of postembryonic development (Barr et al., 2018; Sulston et al., 1980; Sulston and Horvitz, 1977). Sexually dimorphic differentiation in the nervous system falls into two broad types. There are neurons that are present only in one sex but not the opposite sex, either as a result of sex-specific cell death or as a result of sex-specific induction of proliferation and differentiation of ectodermal blast cells during specific larval stages (Sulston et al., 1980; Sulston et al., 1983). Most and perhaps all of these sex-specific neurons are directly involved in several distinct aspects of sex-specific mating and reproductive behavior (Emmons, 2018).

The second type of sexual dimorphisms in the *C. elegans* nervous system are observed within embryonically born, postmitotic neurons that are present in both sexes but

adopt sex-specific features during sexual maturation in later larval stages (Portman, 2017). These features include sexually dimorphic synaptic wiring patterns (Jarrell et al., 2012) and sex-specific expression of signaling molecules, such as neurotransmitters, neuropeptides and chemoreceptors (Hilbert and Kim, 2017; Pereira et al., 2015; Ryan et al., 2014; Serrano-Saiz et al., 2017a; Serrano-Saiz et al., 2017b). Most if not all of these sexually dimorphic features of sex-shared neurons also come into existence at the fourth larval stage. For example, the AIM interneuron class is glutamatergic in juvenile, pre-sexual maturation stages of both sexes, and in the fourth larval stage only males will turn off glutamatergic identity and turn on cholinergic neurotransmitter identity instead (Pereira et al., 2015). In other cases, sexually dimorphic features emerge from a "mixed" juvenile state. For example, juvenile phasmid sensory neurons innervate several distinct interneuron targets in both sexes before sexual maturation, but during sexual maturation specific subsets of these connections get pruned in a sex-specific manner, again during the fourth larval stage (Oren-Suissa et al., 2016). The fourth larval stage is emerging not only as a key stage in which sex-specific features of sex-shared neurons mature into their terminal stage, but it is also the stage at which sex-specific neurons mature to a fully differentiated state. For example, the sex-specific HSN and CEM neurons, even though generated in the embryo, only acquire terminal features (e.g. neurotransmitter identity) in the fourth larval stage (Desai et al., 1988; Pereira et al., 2015; Sulston and Horvitz, 1977). The molecular mechanisms that control the timing of these sexual maturation events in postmitotic neurons of the nervous system have largely remained obscure.

Candidate regulators of these developmental timing events are so-called heterochronic genes, first identified in *C. elegans* (Ambros and Horvitz, 1984). Heterochronies refer to offsets of the relative timing of somatic developmental events versus gonadal developmental events (Slack and Ruvkun, 1997). In heterochronic mutants, the timing of cellular cleavage patterns in postembryonic skin cell lineages is disrupted in a highly stereotyped manner; in some mutants lineage patterning events normally occurring late will occur earlier ("precocious mutants") or specific cell lineage patterning events will be delayed or never occur (Ambros, 1989; Ambros and Horvitz, 1984; Slack and Ruvkun, 1997). Molecular analysis of these heterochronic mutants revealed a gene regulatory pathway, which contains several deeply conserved post-transcriptional regulatory factors at its core, most notably the conserved miRNA *let-7*, the conserved LIN-28 protein, a negative regulator of *let-7* processing, and the RNA-binding, posttranscriptional regulator LIN-41, a key target of the *let-7* miRNA (**Fig.1A**)(Ambros, 1989; Ecsedi et al., 2015; Moss et al., 1997; Reinhart et al., 2000; Slack et al., 2000). While these regulatory factors are well known to control cell division patterns in the ectoderm, their role in postmitotic cell types is much less well defined (Del Rio-Albrechtsen et al., 2006; Hallam and Jin, 1998; Howell et al., 2015; Olsson-Carter and Slack, 2010; Zou et al., 2013).

Within the nervous system, the impact of heterochronic genes on sex-specific differentiation events during sexual maturation at the juvenile to adult transition has been poorly defined. Such a role is not an obvious matter because heterochronic genes do not control timing in all tissues. For example, heterochronic genes are not involved in controlling the timing of gonadal maturation (Ambros and Horvitz, 1984; Euling and Ambros, 1996). Also, the impact of gonadal maturation on the postmitotic maturation of sexually dimorphic nervous system has not been extensively explored and since the control of sexually dimorphic brain differentiation by hormones is a mechanism broadly employed throughout the animal kingdom (Avendano et al., 2017), it remained a viable possibility that factors other than heterochronic genes may control the timing of sexually dimorphic nervous system maturation.

We show here that the gonad does not impinge on several sexual dimorphic differentiation events in *C. elegans*, but that it is rather the phylogenetically conserved core heterochronic pathway genes *lin-28, let-7* and *lin-41* that control the timing of maturation of sexual dimorphisms in many different neuron classes. We show that these broadly expressed timing genes act through distinct cell-specific effector modules, among them a specific isoform of the *lin-29* Zn finger transcription factor and the two DM domain (DMD) containing transcription factors *mab-3* and *dmd-3*. These temporally regulated effector genes are expressed in a sexually dimorphic manner in distinct sets of sex-shared neurons to control specific aspects of sexually dimorphic features and functions. All these regulatory effector genes are phylogenetically conserved. The recently discovered role of mammalian Lin28 and Let7 genes in controlling the timing of puberty onset suggests the emergence of phylogenetically conserved mechanism to control the timing of sexual maturation.

RESULTS

Effects of the heterochronic *lin-28/let-7/lin-41* pathway on neuron-specific sexual maturation

As an entry point to identify the molecular mechanisms required for the correct timing of nervous system sexual maturation, we used the previously described neurotransmitter switch of the AIM interneurons (**Fig.1B-D**), a sex-shared neuron class that is required for mate searching behavior (Barrios et al., 2012; Pereira et al., 2015). A fosmid-based reporter of the *eat-4/VGLUT* vesicular glutamate transporter is expressed during juvenile stages in the AIM interneuron of both sexes. At the onset of sexual maturation, during the fourth larval stage, AIM neurons of the male turn off the glutamatergic gene reporter and turn on expression of fosmid based reporters for the cholinergic genes *unc-17/VACHT* and *cho-1/CHT* (Pereira et al., 2015). The acquisition of AIM cholinergic identity during sexual maturation only in males was confirmed by analyzing the expression of the cholinergic *unc-17/VACHT* locus, tagged with *mKate2* using CRISPR/Cas9 genome engineering (**Fig.S1A**).

Sexual maturation in many animal species is controlled by gonadal hormones (Avendano et al., 2017). In *C. elegans,* the gonad has been shown to be required for the establishment of sex-specific adult behaviors (Arantes-Oliveira et al., 2002; Fujiwara et al., 2016; Kleemann et al., 2008; Lipton et al., 2004). Therefore, we first examined whether signals from the germline or gonad may affect the AIM neurotransmitter switch. We found that neither genetic removal of the germ cells nor laser ablation of gonadal precursor cells (which results in the loss of both gonad and germline) affects the execution of the AIM neurotransmitter switch (**Fig.S1B-C**).

Temporal control of cell lineage decisions during early larval stages in *C. elegans* has been shown to depend on the activity of the evolutionary conserved heterochronic pathway (Ambros and Horvitz, 1984; Moss and Romer-Seibert, 2014; Slack and Ruvkun, 1997). To test if members of the heterochronic pathway were required for the correct timing of nervous system differentiation during sexual maturation, we examined the impact of heterochronic mutants on the male-specific AIM neurotransmitter switch. We observed no defects in the timing of cholinergic gene battery induction in L4 in *lin-4* null mutant animals which controls the timing of L2-specific aspects of cellular patterning (Ambros and Horvitz, 1984) (data not

shown). However, we observed a premature onset of both *unc-17/VACHT* and *cho-1/CHT* expression in AIM neurons of *lin-28* mutant males (**Fig.1B,D**), mirroring the precocious cellular cleavage defects of *lin-28* in epidermal tissues (Ambros and Horvitz, 1984). Matching the precocious induction of cholinergic identity, *lin-28* mutant males also showed a precocious downregulation of the glutamatergic marker *eat-4/VGLUT* in the AIM interneurons (**Fig.1B,D**).

We also found that in males carrying a loss-of-function mutation in the miRNA *let-7*, whose processing is negatively controlled by *lin-28* (Lehrbach et al., 2009), the neurotransmitter switch of the AIM interneurons is eliminated, i.e. male AIM neurons remain glutamatergic (**Fig.1C-D**). Since *let-7* is a repressor of gene expression, the loss of the neurotransmitter switch suggests that *let-7* may normally act to repress a factor that prevents the neurotransmitter switch. We found that *lin-41,* the first of many *let-7* targets to be identified (Slack et al., 2000) encodes this repressor factor. In *lin-41* loss-of-function mutants (*bch28)*, the neurotransmitter switch was prematurely executed, while in *lin-41* gain-of-function mutants (*xe8)*, in which *let-7* is unable to downregulate *lin-41* activity due to a deletion of the *let-7*-binding sites in the *lin-41* 3'UTR (Ecsedi et al., 2015), the neurotransmitter switch of AIM was abrogated and AIM neurons remained glutamatergic (**Fig. 1B,D**).

The heterochronic pathway genes also controlled the onset of differentiation of the male-specific CEM sensory neurons. Even though these neurons are already born in the embryo (and removed by apoptosis in hermaphrodites; (Sulston et al., 1983)), the CEM neurons only fully differentiate at the fourth larval stage (Pereira et al., 2015). By analyzing the expression of cholinergic reporters, we found that this L4-specific maturation event is also precisely timed by the heterochronic pathway genes. In *lin-28* mutants, CEM neurons prematurely expressed cholinergic genes while in *let-7* mutants CEM neurons' terminal differentiation was blocked (**Fig.1E,F**). As we had seen for the AIM neurotransmitter switch, *lin-41* mutants showed precocious cholinergic gene expression in CEM neurons and *lin-41* gain of function mutants (in which *lin-41* expression fails to be downregulated) also fail to show CEM cholinergic gene expression during sexual maturation suggesting that *let-7* miRNA acts through regulating *lin-41* for the correct timing of this process (**Fig.1E,F**). In conclusion, mutant analysis of the heterochronic pathway genes showed that the *lin-28/let-7/lin-41* regulatory pathway is required for the correct timing and for the acquisition of male specific features of two distinct neuron classes.

The *lin-29* Zn finger transcription factor is the relevant target of *lin-41* in controlling the AIM neurotransmitter switch

lin-41 encodes for a versatile regulatory protein with RING and NHL domains, involved in both post-transcriptional RNA regulation (including translation) and protein ubiquitination (Ecsedi and Grosshans, 2013). To ask which of the many previously described effectors of LIN-41 (Aeschimann et al., 2017; Ecsedi and Grosshans, 2013) are relevant in the context of the AIM neurotransmitter switch, we turned to the *lin-29* Zn finger transcription factor, whose expression is translationally inhibited by *lin-41* in the context of timing of skin cell proliferation (Aeschimann et al., 2017; Ambros and Horvitz, 1984; Rougvie and Ambros, 1995; Slack et al., 2000). LIN-29 was previously considered to be an ortholog of the human EGR protein

family, but orthology analysis with several tools (Kim et al., 2018; Wang et al., 2017) as well as a detailed analysis of predicted DNA binding features shows that LIN-29 is rather an ortholog of the uncharacterized vertebrate ZNF362 and ZNF384 proteins (**Fig.2A**). During the larva-to-adult transition, *let-7* inhibition of *lin-41* derepresses *lin-29* expression and induces adult gene expression programs in the epidermis. Consistent with *lin-29* being a functional effector of *lin-41* in the AIM interneurons, we find that the AIM neurotransmitter switch is entirely lost in *lin-29* null mutants (**Fig.1C,D**). In contrast, we found that the onset of differentiation of the male-specific CEM neurons in the L4 stage, as measured by the induction of cholinergic identity, is unaffected in *lin-29* null mutants (**Fig.1E,F**). These findings indicate that *lin-41* controls distinct effector genes in different neuron types.

The transcriptional co-factor *mab-10/NAB* has been shown to act with *lin-29* to control epidermal cell differentiation during the larval to adult transition (Harris and Horvitz, 2011). Moreover, biochemical studies revealed that the *mab-10* transcript, like *lin-29*, is a direct target of regulation by the LIN-41 protein (Aeschimann et al., 2017). By CRISPR/Cas9-mediated tagging of the *mab-10* locus with *mCherry*, we indeed confirmed temporal control of *mab-10* expression (**Fig.S2A**). Like *lin-29,* the expression of *mab-10* starts to be observed at the L4 stage in the nervous system; however, unlike *lin-29*, we find *mab-10::mCherry* to be ubiquitously expressed, including in all neurons, in both sexes. To determine if *mab-10* functions in regulating nervous system differentiation during sexual maturation we analyzed the effects of a newly generated *mab-10* null allele (**Fig.S2A**) for defects in the AIM neurotransmitter switch or CEM cholinergic gene expression. We found that in the absence of *mab-10*, the AIM neurotransmitter switch and the CEM cholinergic gene expression occurred normally (**Fig.1D,F**). This result shows that while *mab-10* functions with *lin-29* in seam cell differentiation, it is not required for *lin-29* function in AIM interneurons in males.

A transition from ubiquitous temporal regulators (*lin-28/let-7/lin-41)* to a sex- and neuron-type specific regulator (*lin-29)*

To address in which cells the heterochronic pathway acts to control the AIM neurotransmitter switch, we examined the expression pattern of *lin-28, let-7, lin-41* and *lin-29* in the nervous system. While expression of these genes in other cells, specifically, the epidermis, has previously been examined in detail (Moss et al., 1997; Rougvie, 2001; Slack et al., 2000), much less is known about their neuronal expression. We analyzed heterochronic gene expression together with either a panneuronally expressed RFP marker or a cholinergic RFP marker (cholinergic labeling of the AIM neuron allowed us to correlate the timing of heterochronic gene expression relative to the AIM neurotransmitter switch). Consistent with previous reporter gene analysis (Moss et al., 1997), we found that a fosmid-based reporter construct of the *lin-28* gene is expressed very broadly in the nervous system in a sexually non-dimorphic manner and downregulated by the end of the L2 stage (**Fig.S2B**).

To analyze *lin-41* expression, we used an endogenously *gfp* tagged *lin-41* allele (Spike et al., 2014). Consistent with previously described expression patterns in the epidermis (Slack et al., 2000), this *lin-41* reporter allele showed broad expression in the nervous system from the L1 until the L4 stage in both sexes, when it is downregulated (**Fig.S2C**). Previous work showed that *lin-41* downregulation in hypodermal tissue depends on *let-7* (Ecsedi et al., 2015; Slack et al., 2000) and to corroborate this notion in the context of the nervous system,

we analyzed *let-7* activity using an "activity sensor" construct in which the *lin-41* promoter is fused to *gfp* and to the *let-7* responsive 3'UTR of the *lin-41* locus. This reporter shows ubiquitous expression, including in the nervous system, from the L1 stage to L4, when GFP levels start to drop and disappear from most tissues, including neurons, by the adult stage (**Fig.S2D**). A control construct carrying the *unc-54* 3' UTR shows it is not normally downregulated at the L4 and young adult stages (**Fig.S2D**). We conclude that *let-7* activity is, as expected, temporally controlled in the nervous system. We did not observe any sexual dimorphisms of *lin-41* or *let-7* sensor expression in the nervous system.

To determine the expression pattern of the *lin-41* effector *lin-29* in the nervous system, we used strains in which the *lin-29* locus was tagged with *gfp*, using CRISPR/Cas9-mediated genome engineering. *lin-29* produces two distinct transcripts, *lin-29a* and *lin-29b* that differ at their 5'end; both contain five DNA-binding Zn finger domains (Rougvie and Ambros, 1995)(**Fig.2A**). We use a strain in which both isoforms were simultaneously tagged by introducing *gfp* at the 3' end of the locus (Aeschimann et al., 2017). In addition, we examined the expression pattern exclusively of the *b*-isoform, by introducing the same 3' terminal tag in the *a*-isoform-specific allele (*xe40*) via CRISPR/Cas9-mediate genome engineering (**Fig.2A**). To examine the expression pattern of the *a*-isoform, we inserted *gfp* at the 5' end of the *a*-isoform (**Fig.2A**). Generally, the expression pattern of the *gfp* allele that tags both isoforms matches the expression pattern reported using an antibody directed against both LIN-29 isoforms (Bettinger et al., 1996; Euling et al., 1999). As previously reported, we observed expression in head neurons and the ventral nerve cord. However, we found that this neuronal expression is almost completely restricted to the male and this male-specific expression can be entirely ascribed to the *a*-isoform (**Fig.2B**). The male-specific neuronal expression of *lin-29a* is not observed in male-specific neurons but is, interestingly, entirely restricted to sex-shared neurons (i.e. neurons that are generated in both sexes). Intriguingly, most of these neurons had not been previously reported to show sexually dimorphic gene expression patterns or functions. Specifically, 24 out of 116 sex-shared neuron classes express *lin-29a,* including five sensory neuron classes in the head and tail (AWA, ASG, ASJ, ASK, ADF, PHB, PLM), seven interneuron classes (AVA, RIA, AIM, AVG, RIF, PVC, PVN), a few head and tail motor neurons (SAB, PDA, PDB) and most of the sex-shared ventral nerve cord motor neurons (dorsal and ventral A, B and D-type and AS neurons). Many of these LIN-29 expressing neurons are synaptically connected to one another (White et al., 1986) and some of the synaptic connections are known to be sexually dimorphic (Jarrell et al., 2012).

Expression of *lin-29a* in all these neurons in the male nervous system is precisely temporally controlled; it is first observed in the early L4 stage and persists throughout adulthood. In addition to the male-specific neuronal expression of the *lin-29a* isoform, we also found that the *lin-29b* isoform is expressed in 3 postembryonically generated touch neurons (AVM, PVM, PDE), where its expression is not temporally regulated, i.e. its expression is induced right after the neurons are born in the first two larval stages and expression is observed in both sexes.

The late larval onset of expression of *lin-29* in non-neuronal cells has been reported to be controlled by the heterochronic pathway (Bettinger et al., 1996; Moss et al., 1997). To assess whether onset of male-specific, neuronal expression of the *lin-29a* isoform is controlled by *lin-41* and *let-7*, we analyzed *lin-29a* neuronal expression in these mutant backgrounds. Indeed, we found that in *lin-41(lf)* mutants *lin-29a::gfp* expression is observed

prematurely including in the sex-shared neurons of the male (**Fig.S4A**). As expected, in *let-7(lf)* and *lin-41(gf)* mutants (both of which maintain expression of LIN-41), *lin-29a::gfp* expression levels are significantly reduced compared to wild type adult males (**Fig.S4B**). This decrease in *lin-29a* expression is consistent with the similarity of loss of function phenotypes of *let-7* and *lin-29* null mutants and *lin-41* gain of function mutant where the AIM neurotransmitter switch does not occur (**Fig.1**). Together with our previous biochemical analysis (Aeschimann et al., 2017), we conclude that *let-7*-controlled LIN-41 directly represses *lin-29a* translation to control the precise timing of LIN-29A protein accumulation in the nervous system.

The *lin-29a* isoform is required cell-autonomously and is sufficient to define male-specific neurotransmitter switch in the AIM interneuron

To validate the functional relevance of the *lin-29a* isoform in controlling the AIM neurotransmitter switch, we generated two *lin-29a*-isoform specific alleles (*xe38* and *xe40*) using CRISPR/Cas9 genome engineering (**Fig.2A).** We indeed find that in both isoform-specific alleles the male-specific AIM neurotransmitter switch failed to occur (**Fig.3A**). A newly generated *lin-29* null allele that removes both isoforms also confirmed the results previously reported with the canonical null alleles tested (**Fig.3A**).

To assess whether *lin-29a* acts cell-autonomously in AIM to control its neurotransmitter switch, we expressed *lin-29a* under an AIM-specific promoter (Serrano-Saiz et al., 2017a). This driver is not only active in both sexes, but it is already active in embryos and early larval stages, hence allowing us to assess three key issues: (1) whether LIN-29A acts cell-autonomously, (2) whether LIN-29A can induce the neurotransmitter switch prematurely in males and (3) whether LIN-29A can ectopically induce the AIM neurotransmitter switch in neurons of hermaphrodites. We generated two independent transgenic lines that cell type-specifically express *lin-29a* in a *lin-29a (xe38 and xe40)* mutant background. We found that in adult male animals, the loss of the AIM neurotransmitter switch (as assayed by *cho-1* and *unc-17* induction and *eat-4* downregulation in AIM) is rescued by the transgene, thereby demonstrating cell autonomy of LIN-29A function (**Fig.3B**).

Examining juvenile males, before the onset of overt sexual maturation, we observed that the neurotransmitter switch is executed prematurely already by the first larval stage in these transgenic animals ectopically expressing LIN-29A in AIM neurons (**Fig.3B**). This sufficiency experiment indicates that the temporal control of *lin-29a* expression, and specifically the repression of *lin-29a* by the heterochronic pathway is required to prevent *lin-29a* from triggering the neurotransmitter switch precociously. Lastly, examining adult hermaphrodite animals expressing this construct, we found that *lin-29a* is sufficient to induce the neurotransmitter switch in the opposite sex (**Fig.3B**). We conclude that *lin-29a* is required and sufficient to control the AIM neurotransmitter switch.

To assess whether *lin-29a* function in AIM goes beyond controlling AIM's neurotransmitter switch, we examined another molecular marker of sexually dimorphic AIM differentiation, the orphan GPCR, *srj-54*, which is induced in the AIM neurons upon male sexual differentiation (Portman, 2007). We found that *srj-54* fails to be expressed in *lin-29a* mutants (**Fig.4A**) adding another AIM male-specific molecular feature that fails to be normally induced in the absence of *lin-29*. As we will describe further below, *lin-29a* mutants are also

defective in an AIM-mediated sexual behavioral paradigm.

lin-29a controls sexually dimorphic molecular features of other sex-shared neurons.

The expression of *lin-29a* in a number of distinct neuron types indicated that *lin-29a* may play additional roles in controlling sexually dimorphic, i.e. male-specific nervous system features. To this end, we assessed two other molecular markers that were previously found to be expressed in a sexually dimorphic manner in two distinct, sex-shared neuron classes, both of which express *lin-29a*. First, the *dmd-5* transcription factor was reported to be expressed in AVG neurons in adult males but not in hermaphrodites (Oren-Suissa et al., 2016). By analyzing the expression of a *dmd-5* reporter in *wild type* versus *lin-29a* mutants we found that *lin-29a* is required for *dmd-5* expression in AVG in males (**Fig.4B**). Second, the *daf-7* gene, encoding a neuroendocrine TGFβ-like signal, is turned on during sexual maturation in the sex-shared ASJ neurons only in males (Hilbert and Kim, 2017). This induction is also abrogated in *lin-29a* mutants (**Fig.4B**). Non-dimorphic expression of *dmd-5* and *daf-7* in other neuron types was not affected by *lin-29a.*

The electron micrographical reconstruction of the nervous system of *C. elegans* male revealed sexually dimorphic neuronal morphology and connectivity of several sex-shared neurons (Jarrell et al., 2012; White et al., 1986). Specifically, the *lin-29a*-expressing PDB motorneuron located in the pre-anal ganglion, grows elaborate branches off from its cell body and initial segment of its posteriorly directed main process. This was only observed in the male but not in the hermaphrodite (Jarrell et al., 2012; White et al., 1986). These male-specific branches make extensive chemical and electrical synaptic contacts with both male-specific neurons, as well as sex-shared neurons (Jarrell et al., 2012). We corroborated the existence and reproducibility of male-specific branches by visualizing PDB with a reporter transgene (**Fig.4C**). We found these branches grow specifically during sexual maturation in the L4 stage (**Fig.4C**), co-incident with the onset of *lin-29a* expression. Growth of these branches is disrupted in *lin-29a* mutants (**Fig.4C**). These findings demonstrate a role for *lin-29a* in regulating the temporal and sexually dimorphic acquisition of male-specific neuronal morphologies and predict that PDB fails to make its branch-specific synaptic contacts in the absence of *lin-29a*. We conclude that *lin-29a* affects multiple distinct types of sexual maturation events, from gene expression to anatomy, in distinct neuron classes.

Feminization of the behavioral patterns of *lin-29a* mutant males

We next sought to broaden our understanding of *lin-29a* function in the nervous system by testing if it was required for the establishment of adult-specific sexually dimorphic behaviors. Critical for such an analysis is the fact that *lin-29a* mutant males do not display the obvious morphological and patterning defects displayed by the *lin-29* null allele. Specifically, the male tail, whose overall morphogenesis is disrupted in *lin-29* null mutants (Euling et al., 1999) appears morphologically normal in *lin-29a* mutants (**Fig.S5A**). We precisely quantified other morphological differences between hermaphrodites and males using an automated visualization/measurement tool (Yemini et al., 2013) and found no morphological differences between wild-type and *lin-29a* mutant animals (**Fig.S5B**). The normal overall appearance of *lin-29a* mutant males allowed us to first ask whether *lin-29a* mutant males displayed mating-related behavioral defects. One aspect of mate attraction relates to the mating process itself,

in which the male detects various sensory cues from the hermaphrodites to engage in direct contact (Liu and Sternberg, 1995). Previous work with the *lin-29* null mutant revealed multiple defects in these direct interactions and these defects were ascribed to spicule patterning defects (Euling et al., 1999). In spite of spicule patterning appearing normal in *lin-29a* isoform-specific mutants, we observed that these mutants were unable to mate (**Fig.5A**). We found that one aspect of mate behavior that is defective in these mutants is vulva location behavior (**Fig.5A**).

The AIM and ASJ neurons, both of which express *lin-29a* specifically in males, were previously implicated in mate-searching, which is another aspect of mating behavior (Barrios et al., 2012; Hilbert and Kim, 2017). In this behavioral paradigm, well-fed single adult males leave a source of food to explore their environment in search for mating partners. We indeed found that *lin-29a* mutants are defective in mate searching behavior (**Fig.5B**). These defects are similar to the defects caused by loss of *daf-7/TGFβ* (Hilbert and Kim, 2017) and, consistent with this phenotypic similarity, we had described above that *daf-7/TGFβ* expression is lost in the ASJ neurons of *lin-29a* mutants. However, we noted that we could partially rescue the mate searching defects of the *lin-29a* mutant males by restoring LIN-29A expression exclusively in the AIM neurons (**Fig.5B**), indicating that *lin-29a* may function in several distinct neurons to control mate searching behavior.

The male-specific expression of *lin-29a* in ventral nerve cord and head motor neurons and in a command interneuron pair made us consider whether *lin-29a* may be involved in controlling aspects of sexually dimorphic locomotor behavior. It has previously been shown that adult male and hermaphrodites display distinct locomotor behavior when crawling on a lawn of bacteria (Mowrey et al., 2014). We extended the analysis of sexually dimorphic adult-specific behavior using an automated worm tracker system which quantifies several hundred distinct postural and locomotory features of an animal (Yemini et al., 2013). We found a large number of sexually dimorphic features. While many of them were not affected in *lin-29a* mutant animals (**Fig.5C and TableS1**), we found that *lin-29a* mutants displayed a striking feminization of a number of body posture and locomotory features. Postural differences included head bend, neck bend, midbody bend, hips bend, amplitude ratio and primary wavelength. (**Fig.5C**). Other *lin-29a*-dependent locomotory features included midbody crawling amplitude and tail crawling amplitude (**Fig.5C**). The lack of morphological differences between wild-type and *lin-29a* mutant males indicate that these locomotory phenotypes are the result of neuronal defects rather than being a secondary consequence of overall body morphology. Taken together, these results show that *lin-29a* is required for the acquisition of male-specific postural and locomotory features and that the absence of *lin-29a* results in a feminization of these behavioral parameters.

We sought to determine in which of the neurons that express *lin-29a* in a sexually dimorphic manner *lin-29a* acts to control aspects of the locomotor behaviors described above. We particularly considered the so-called “motor circuit”, composed of a set of command interneurons and ventral nerve cord motor neurons (Von Stetina et al., 2006). Expression of *lin-29a* in the motor circuit, using a *cis*-regulatory element from the *unc-17/VAChT* locus rescued a defined subset of the feminized behavioral feature (wavelength, crawling amplitude and midbody bend) (**Fig.5C**). Other *lin-29a*-expressing neurons may be involved in controlling locomotory features not rescued by this transgene.

Intersectional control of the temporal, sexual and spatial specificity of *lin-29a* expression

Having established the function of *lin-29a* in sexually dimorphic development and function of the *C. elegans* nervous system, we sought to better understand the mode of *lin-29a* regulation. *lin-29a* shows a striking specificity of expression in three different dimensions. It is expressed in a temporally controlled manner (onset in embryonically born neurons only in the L4 stage), in a sex-specific manner (only in males) and it is expressed in a highly neuron type-specific manner. In as far as the first dimension, time, is concerned, we have already shown above that *lin-29a* expression in the nervous system is temporally controlled by the *lin-28/let-7/lin-41* heterochronic pathway. To assess the control of sex-specificity of *lin-29a* expression, we genetically removed *tra-1,* the master regulatory transcription factor of sex determination which is normally expressed in all hermaphroditic cells (XX sex chromosome genotype) where it suppresses male identities. We found that in *tra-1(e1488)* mutants, *lin-29a* expression becomes derepressed in XX animals (**Fig.6A**). To assess focus of action of *tra-1*, we induced the degradation of *tra-1* exclusively in the nervous system by force-expressing *fem-3*, which promotes TRA-1 protein destruction (Starostina et al., 2007), under the control of a panneuronal driver. We found that *lin-29a* expression is derepressed in the nervous system of the hermaphrodite, with the same pattern of cellular specificity seen normally in males (**Fig.6A**).

To address the cellular specificity of *lin-29a* expression, we considered the possibility that neuron class-specific terminal selector-type transcription factors that control the expression of neuron-class specific identity programs (Hobert, 2016) may also control the neuronal specificity of *lin-29a* expression. For example, the terminal differentiation program of the *lin-29a* expressing ASK neurons is controlled by the LIM homeobox gene *ttx-3/LHX2* and the identity of the AIM neuron is defined by the *unc-86/BRN3* POU homeobox gene (Serrano-Saiz et al., 2013). We found that *lin-29a* expression is eliminated in the ASK neurons of *ttx-3* mutants and in the AIM neurons of *unc-86* mutants (**Fig.6B**). The *unc-3*/COE-type transcription factor controls the identity of multiple neurons of the motor circuit, including the *lin-29a* expressing ventral nerve cord motorneurons, the SAB head motor neurons, the PDA and PDB tail motor neurons and the command interneurons AVA and PVC (Kratsios et al., 2011; Pereira et al., 2015). We found that in *unc-3* mutants *lin-29a* expression is lost in all these neurons (**Fig.6B**). We conclude that the complex *lin-29a* expression pattern can be explained by an intersectional mechanism. Temporal control is exerted via the heterochronic pathway, sexual specificity by the sex determination pathway and cellular specificity by terminal selector-type neuronal identity factors.

Other male-specific effectors of *lin-41* are also controlled in an intersectional manner

The sexually dimorphic expression pattern of *lin-29a* in the male nervous system does not extend to all sex-shared neurons that are known to display sexually dimorphic features. For example, the sex-shared PHC sensory neuron functionally and anatomically remodels during sexual maturation (Serrano-Saiz et al., 2017a), but does not express *lin-29a.* This suggests that *lin-29a* is possibly just one of several targets of LIN-41 in the context of male-specific nervous system differentiation. Previous whole animal RNA profiling of *let-7* and *lin-41* mutants, as well as RNA binding assays demonstrated that LIN-41 also represses *mab-3*

and *dmd-3* mRNA (Aeschimann et al., 2017). Both genes are members of the DMD family of sex-specifically expressed transcription factors (Mason et al., 2008; Yi and Zarkower, 1999). Both genes were previously shown to be expressed in a male-specific manner in non-neuronal somatic tissue, in male-specific neurons and in a male-specific manner in distinct, but sex-shared neurons (Mason et al., 2008; Serrano-Saiz et al., 2017a; Yi et al., 2000). Their timing of expression had not been previously examined.

We *gfp*-tagged the endogenous *mab-3* and *dmd-3* loci using CRISPR/Cas9 genome engineering. Within the sex-shared nervous system, we found that *mab-3* is not only male-specifically expressed in the ADF neuron, as previously reported (Yi et al., 2000), but also in additional head neurons, including the embryonically generated SMD head motor neurons (**Fig.6C**). We found that like the male-specific, neuronal expression of *lin-29a*, male-specific SMD expression of *mab-3* is precisely timed to commence at the L4 stage (**Fig.6C**). Similarly, the *gfp*-tagged *dmd-3* locus is expressed in a sex-shared neuron class, the PHC neurons **(Fig.6D)**, where *dmd-3* acts to control the sexually dimorphic remodeling of PHC (Mason et al., 2008; Serrano-Saiz et al., 2017a). *dmd-3::gfp* expression in PHC also commences at the L4 stage **(Fig.6D)**, at the time when PHC neurons remodel in a male-specific manner (Serrano-Saiz et al., 2017a). We corroborated our previous data of LIN-41 protein translationally regulating *mab-3* and *dmd-3* by showing that the temporal specificity of nervous system expression of *mab-3* is indeed lost in *let-7* mutants (**Fig.6C-D**).

Like *lin-29a,* the male-specificity of *mab-3* and *dmd-3* expression is controlled by the *tra-1* transcription factor (**Fig.6E,G**)(Mason et al., 2008; Yi et al., 2000). Lastly, the neuronal specificity of *mab-3* and *dmd-3* expression is, like *lin-29a*, also controlled by neuron-type specific terminal selectors. *unc-42* is a terminal selector transcription factor that controls terminal differentiation of the RMD and SMD neurons (Pereira et al., 2015) and we found that *mab-3* expression in these neurons fails to be induced in an *unc-42* mutant background (**Fig.6C**). Similarly, *ceh-14* is a terminal selector of PHC neuron identity (Serrano-Saiz et al., 2017a) and is required for *dmd-3* expression in PHC (**Fig.6F**). We conclude that *lin-41* operates through multiple distinct, male-specific effector genes and that the temporal, sexual and spatial specificity of expression of these distinct effectors is controlled by a similar, intersectional regulatory logic (**Fig.7A,B**).

DISCUSSION

We have described here that the timing of multiple distinct, neuron-type specific sexually dimorphic maturation events in the nervous system of *C. elegans* are controlled by a phylogenetically conserved regulatory cassette composed of ubiquitously expressed and temporally controlled genes, *lin-28* (a regulator of *let-7* miRNA processing)*, let-7* (a miRNA) and its target *lin-41* (a translational regulator). The conservation of the deployment of this pathway in the timing of sexual maturation is remarkable. Both genetic studies in mice, as well as genetic association studies of humans with abnormally timed puberty demonstrate that *lin-28* and *let-7* also control timing of sexual maturation (puberty) onset in mammals (Chen et al., 2017; Corre et al., 2016; He et al., 2009; Ong et al., 2009; Perry et al., 2009; Sulem et al., 2009; Zhu et al., 2010). This conclusion was further corroborated by the finding that mutations in human makorin, the orthologue of *lep-2*, a regulator of *lin-28* activity in *C. elegans* (Herrera et al., 2016), also affect the timing of puberty (Abreu et al., 2013; Bulcao Macedo et al., 2014). Similarly, in the fly nervous system, *lin-28* and *let-7* are involved in controlling the timing of pupal to adult transitions (Gonzalez-Itier et al., 2018; Sempere et al., 2003; Wu et al., 2012) that are accompanied by sexual maturation in the nervous system, as assessed by expression of the male-specific isoform of Fruitless, a master regulator of male-specific nervous system differentiation (Lee et al., 2000). A regulatory linkage between the heterochronic pathway and transcriptional regulators of sexual differentiation (hormone receptors in vertebrates or Fruitless in flies) has not yet been established in these systems.

Apart from suggesting a remarkable conservation of timing mechanisms of sexual maturation, we have provided insights into the mechanisms by which the *lin-28/let-7* module affects the timing of sexual maturation. The *let-7* miRNA is known to have a plethora of distinct mRNA targets (Bussing et al., 2008; Grosshans et al., 2005), but the one that we define here as being relevant in the context of sexual maturation is the translational regulator *lin-41* (Slack et al., 2000). *C. elegans lin-41* had previously been implicated as the key output of *let-7* in the timing of skin cell maturation events (Slack et al., 2000) as well as vulval patterning (Ecsedi et al., 2015). *lin-41* is also highly conserved in vertebrates where its expression appears to be temporally regulated during embryogenesis with its expression being complementary to *let-7,* as observed in *C. elegans* (Schulman et al., 2005). The dynamics of *lin-28, let-7* and *lin-41* expression has not yet been comprehensively examined in the context of sexual maturation in the vertebrate brain, but notably, the expression of Lin28 and Let7 in the hypothalamus, a site of release of peptides that control pubertal onset, appears to be temporally controlled (Sangiao-Alvarellos et al., 2013). In *Drosophila*, *let-7* expression has also been found to be temporally regulated; its expression increases during late pupal stages (Faunes and Larrain, 2016). This is the time at which at least some parts of the *Drosophila* nervous system sexually mature (Lee et al., 2000), but a role of *Drosophila let-7* in the timing of sexual maturation has not yet been assessed.

We showed here that the key target of *let-7*, the *lin-41* translational regulator, relays temporal information in a modular manner to distinct, neuron class-specific outputs (**Fig.7A**). Among them is the phylogenetically conserved LIN-29 Zn finger transcription factor (whose vertebrate orthologs ZNF362 and ZNF384 are completely unstudied), which we identified as a sexually dimorphically expressed factor, present in one fifth of all sex-shared neuron classes. Two other targets of *lin-41* that are relevant for sexual maturation are two male-specifically expressed DM domain transcription factors (Aeschimann et al., 2017)(this paper).

Neurons that express these sexually dimorphic output regulators (*lin-29, mab-3, dmd-*3) act at distinct levels of information processing, from sensory, to inter- to motorneurons. Intriguingly, many of the sex-shared, LIN-29(+) interneurons are synaptically connected and some of these connections are sexually dimorphic. Some of the neurons that express LIN-29 or MAB-3 in a male-specific manner were not previously shown to display any sexual dimorphisms, demonstrating that the *C. elegans* nervous system may be even more sexually dimorphic than previously appreciated.

lin-29, mab-3 and *dmd-3* expression mark many, but not quite all sex-shared neurons with sexually dimorphic features. We indeed found evidence for two other *dmd* genes whose expression is both sexually and temporally controlled in yet distinct neuron classes (Oren-Suissa et al., 2016)(unpubl. data). Altogether, these findings suggest a scenario in which a ubiquitously expressed temporal coordinate system (heterochronic pathway), intersects with a ubiquitously expressed sexual coordinate system (sex determination pathway) to control the sexual and temporal specificity of a number of modular, neuron-type specific output systems that control sexual dimorphisms in distinct cellular circuit modules (**Fig.7A,B**). This modular organization displays striking conceptual similarities with the modular organization of sexual dimorphic control mechanisms in vertebrates (Yang and Shah, 2014).

How is the neuron type-specificity of the modular outputs (*lin-29, mab-3, dmd-3* etc.) of the temporal and sex-determination system controlled? We provided evidence here that the neuron-type specificity of the sex-specific regulator is controlled by neuron-type specific terminal selector transcription factors which define the overall differentiated state of individual neuron classes (Hobert, 2016)(**Fig.7B**). For example, *unc-3* is required for many (non-sexually dimorphic) aspects of motor neuron differentiation in the ventral nerve cord and we find that *unc-3* also is required to target *lin-29* expression specifically in ventral nerve cord neurons. Like the regulation of *lin-29* by the temporal cue *lin-41*, the neuron-type specific regulation of *lin-29* could potentially be direct since we noted several phylogenetically conserved binding sites for UNC-3 protein in the *lin-29* locus. The regulation of sex-specific output regulators, like *lin-29*, by terminal selectors reveals the potential existence of a specific gene regulatory network architecture. For example, in the male AIM neurons, *unc-86* and *ceh-14* are required for the induction of *unc-17* and *cho-1* expression (Pereira et al., 2015). Both are apparently not sufficient to induce *unc-17* and *cho-1* expression in hermaphrodites, but via the *unc-86*-mediated induction of *lin-29* expression in the AIM neurons in males, *unc-86* and *ceh-14* are now apparently able to induce, with the help of *lin-29*, the expression of *unc-17* and *cho-1*. Further biochemical studies will be required to corroborate the existence of such feedforward architecture (**Fig.7B**). In conclusion, we have identified an intersectional regulatory mechanism in which temporal cues, sexual cues and neuron-type specific cues define the onset of expression of sex-specific, neuron-type specific “output regulators” which define sexual dimorphic features of the *C. elegans* nervous system (**Fig.7**).

ACKNOWLEDGEMENTS

We thank Qi Chen for generating transgenic strains, Emily Bayer for generating and providing a *ceh-14* null allele, Bob Horvitz and Hannes Bülow for providing strains and DNA, and members of the Hobert lab for comments on the manuscript. We thank Iskra Katic, Land Xu, Magdalene Rausch and Chiara Azzi for their help in generating strains. This work was supported by the NIH (2R37NS039996 to O.H.), by a Birch/Derchin Fellowship to C.W, by the Swiss National Science Foundation (grant 31003A_163447 to H.G.) and by the Novartis Research Foundation through FMI (to H.G.) and the Howard Hughes Medical Institute (O.H.).

EXPERIMENTAL PROCEDURES

C. elegans strains

The worm strains used in this study are listed in Table S2. The wild type strain was Bristol N2. Worms were grown on nematode growth media (NGM) seeded with bacteria (OP50) as a food source. To synchronize worms 10 adult gravid hermaphrodites were transferred to a new plate with OP50. Worms were allowed to lay eggs for approximately two hours and adult gravid hermaphrodites were removed afterwards. Transgenic lines carrying extrachromosomal arrays were generated by germline injection with 20ng/ul of plasmid DNA and *unc-122::gfp* as a co-injection marker, also at 20ng/ul.

Laser ablation

Laser ablation of Z1/Z4 was performed at the L1 stage as previously described (Hsin and Kenyon, 1999). A MicroPoint Laser System Basic Unit (N2 pulsed laser (dye pump), ANDOR Technology) attached to a Zeiss Axio Imager Z2 microscope (Objective EC Plan-Neofluar 63X/1.30 Oil). Worms were recovered by washing with M9 buffer and imaged at the young adult stage. Control animals were treated in the same manner, but not subjected to laser exposure. Gonad and germline removal were confirmed by DIC.

Microscopy

Worms were anesthetized using 100mM of sodium azide and mounted on 5% agarose on glass slides. All images were acquired using a Zeiss confocal microscope (LSM880; Zeiss [Carl Zeiss], Thornwood, NY). Image reconstruction was performed using the ZEN software tool. Maximum intensity projections of representative images are shown.

Genome engineering

Isoform-specific gfp::3xflag tagging of endogenous lin-29 using CRISPR-Cas9. In order to obtain the *lin-29(xe65)* allele, specifically tagging *lin-29b* at the C-terminus, the following mix was injected into *lin-29a(xe40)* mutant worms: 50 ng/µl pIK155, 100 ng/µl of pIK198 with a cloned sgRNA (atattatttatcagtgattg), 2.5 ng/µl pCFJ90, 5 ng/µl pCFJ104 and 10 ng/µl pFA26 (pDD282 with cloned homology arms). Recombinants were isolated according to the protocol by Dickinson *et al*. (Dickinson et al., 2015), verified by DNA sequencing and outcrossed three times. The plasmid for homologous recombination (pFA26) was previously described (Aeschimann et al., 2017). The *lin-29(xe63)* allele specifically tags *lin-29a* with GFP::3xFLAG at the N-terminus (Aeschimann et al., in preparation).

Tagging of endogenous mab-10 with flag::mCherry using CRISPR-Cas9. In order to tag *mab-10* with *flag::mCherry* at the C-terminus, the following mix was injected into *unc-119(ed3)* worms (Dickinson et al., 2015; Katic et al., 2015): 25 ng/ul pIK155, 65 ng/ul of pIK198 with a cloned sgRNA (gctcccggaatcttgaagct), 10 ng/ul pIK127 (Peft-3::gfp::h2b), 5 ng/ul Pmyo-3::gfp and 65 ng/ul pIK284. The plasmid serving as a template for homologous recombination (pIK284) was obtained using the SapTrap protocol (Schwartz et al., 2016), by combining SapTrap component vectors pMLS257, pMLS291 and pMLS382 with two pairs of annealed oligos (oIK1052/oIK1053, oIK1054/oIK1055). Wild-type moving recombinants were isolated, verified by DNA sequencing and outcrossed three times. The *mCherry* tag of the *mab-10::mCherry* allele is not fully functional as *mab-10(xe75)* and *mab-10(xe44)* both enhance the bursting phenotype of *let-7(n2853)* (data not shown).

lin-29, *lin-29a* and *mab-10* null mutant alleles. In order to specifically mutate *lin-29a* without affecting expression of *lin-29b*, we introduced deletions into the coding exons specific to *lin-29a*, at the same time introducing a frame-shift in the downstream *lin-29a* reading frame. The *lin-29a(xe38)* allele is a 10 bp deletion in exon 2, resulting in a frame-shift and a stop codon in exon 3. It was obtained by injecting a single sgRNA (gctggaaccaccactggctc) and has the following flanking sequences: 5' gaatagctggaaccaccact – *xe38* deletion – ctaccacccattttggtgtt 3'. The *lin-29a(xe40)* allele is a 1102 bp deletion covering exons 2-4, introducing a frame-shift in the *lin-29a* reading frame with a predicted stop codon in exon 6 (Aeschimann et al., in preparation). We used deletions of almost the entire coding regions as null alleles for *lin-29* and *mab-10*: The *lin-29(xe37)* allele is a 14.8 kbp deletion spanning *lin-29* exons 2-11 and the *mab-10(xe44)* allele is a 2.9 kbp deletion spanning *mab-10* exons 3-9 (Aeschimann et al., in preparation).
To obtain mutant worm lines, wild-type worms were injected with a mix containing 50 ng/µl pIK155, 100 ng/µl of each pIK198 with a cloned sgRNA, 5 ng/µl pCFJ90 and 5 ng/µl pCFJ104, as previously described (Katic et al., 2015). Single F1 progeny of injected wild-type worms were picked to individual plates and the F2 progeny screened for deletions using PCR assays. After analysis by DNA sequencing, the alleles were outcrossed three times to the wild-type strain.
Tagging of endogenous unc-17 with 3xflag::mKate2 using CRISPR-Cas9. The *unc-17* locus was tagged at the C-terminus as previously described (Dickinson et al., 2015; Katic et al., 2015).The plasmid serving as a template for homologous recombination was cloned using Gibson and included 700 bp-long homology arms. Wild-type moving recombinants were isolated, verified by DNA sequencing and outcrossed three times.
Tagging of endogenous mab-3 and dmd-3 with 3xflag::gfp using CRISPR-Cas9. The *mab-3* and *dmd-3* loci were tagged at the C-terminus as previously described (Dickinson et al., 2015; Katic et al., 2015).The plasmid serving as a template for homologous recombination was cloned using Gibson and included 700 bp-long homology arms. Wild-type moving recombinants were isolated, verified by DNA sequencing and outcrossed three times.

Transgenic strains
The *kal-1 gfp* promoter fusion corresponds to 'promoter G' from (Wenick and Hobert, 2004). *srj-54::yfp* is a PCR fragment that was constructed using standard PCR SOEing methods by fusing fragment A, comprising 664 bp upstream of the predicted ATG of *srj-54* and the first four codons of *srj-54* coding sequence, to fragment B, comprising *yfp* fused to the *unc-54* 3´ UTR. *srj-54::yfp* was injected with *unc-122::gfp* into *him-5(e1490)* to generate a stable extrachromosomal array. This array was integrated into the genome using standard UV irradiation methods followed by several rounds of backcrossing to *him-5(e1490)* to generate *fsIs5*. For neuron-specific expression, promoter constructs driving *lin-29a* cDNA were generated by Gibson assembly or RF cloning. cDNA was amplified from pDH06, kindly provided by Dr. Horvitz (Harris and Horvitz, 2011). A 1kb of the *unc-17/VACHT* promoter that drives expression in AVA, SAB, DA, DB, VA, VB, PDA and PDB neurons (our unpublished data) was amplified by PCR from the fosmid construct (FW AATGAAATAAGCTTGCATGGTATACACCAATCATTTCTCC and REV TCCTCTAGAGTCGACCTGCAGATAATTTAATTAAAATTGAGTTCCAAC). The PCR fragments were assembled into pPD95.75 by Gibson. For AIM-specific expression a fragment of the *eat-4* locus was used to drive LIN-29A expression. The *lin-29a* cDNA was inserted to replace the *fem-3* cDNA in this construct (Pereira et al., 2015). For nervous system masculinization, a *rab-3* pan-neuronal promoter driving *fem-3::mCherry* was used (White et

al., 2007).

Neuron identification

Expression analysis for the *lin-29* endogenously tagged alleles to a neuron-specific resolution was done by Nomarski optics and crossing these strains with neuronal landmark reporter strains *eat-4 (otIs518) (*Serrano-Saiz et al., 2017a) and *cho-1 (otIs544)* (Pereira et al., 2015).

Neurite tracing

Confocal *Z*-stacks were opened using FIJI, and loaded into the Simple Neurite Tracer plugin. All neurites emerging from the soma or posterior process of PDB were traced. The simple neurite tracer plugin was used to analyze the skeletons for neurite length, which were summed to calculate total neurite.

Mating assays

Animals were synchronized at the L1 stage and grown to the early L4 stage group housed. The day before the mating assay experiment, males at the early L4 stage were separated to a new plate. Male mating behavior was assayed by direct observation of the mating process. A single young adult male was placed with 10-15 L4 *unc-3(e151)* hermaphrodites on a mating plate. The male mating behavior was recorded as previously described (Euling et al., 1999). Males were tested for their ability to locate vulva in a mating assay, calculated as location efficiency. The number of passes or hesitations at the vulva until the male firs stops were counted: location efficiency = 1/number of encounters to stop, expressed as percentage.

Mate-searching assay

Animals were synchronized at the L1 stage and grown to the early L4 stage group housed. The day before the mating assay experiment, hermaphrodites and males at the early L4 stage were separated to a new plate. The mate-searching assay was performed as previously described (Lipton et al., 2004). A single animal was placed in the center of a 15*ul* patch of food per 10 cm plate. Each animal that had left the food was scored blindly at 7 time points for a period of 24 hours. A worm was considered a leaver if at the scoring time it was 3cm away from the food source.

Automated worm tracking

Automated single worm tracking was performed using Wormtracker 2.0 system at room Temperature (Yemini et al., 2013). Animals were synchronized at the L1 stage and grown to the early L4 stage group housed. The day before the tracking experiments, hermaphrodites and males were separated to same-sex group housed plates. Animals were recorded at the young adult stage for 5 minutes to ensure sufficient sampling of locomotion related behavioral features. All animals were tracked on NGM plates uniformly covered with food (OP50). To avoid potential variability arising due to room conditions, all strains that were compared in a single experiment were recorded simultaneously in identical room condition, along with the controls. Analysis of the tracking videos was performed as previously described (Yemini et al., 2013). After correction for multiple testing (Bonferroni correction), features shown in Fig. 5 and Table S1 immerged as the ones with most significantly different q-value among the test groups. For the rescue experiment we only measured these features, permitting us to use the p-value.

FIGURE LEGENDS

Figure 1. Heterochronic pathway effects on AIM and CEM neuronal differentiation during sexual maturation.

A: A simplified schematic of the heterochronic pathway, deduced from the genetic analysis of hypodermal cell lineage division events. The LIN-28 RNA binding protein prevents the maturation of miRNA *let-7*. When LIN-28 protein levels go down at the end of the second larval stage (L2), mature miRNA *let-7* levels rise and bind to the 3'UTR of *let-7* targets. One *let-7* target is the RNA-binding protein LIN-41, whose levels are downregulated at the onset of sexual maturation (L4). This allows for its negative regulator, the zinc-finger transcription factor *lin-29,* to be expressed at the L4 stage to induce the larval to adult transition.
B: AIM neuronal differentiation is precocious in *lin-28(lf)* and *lin-41(lf)*. *unc-17/VACHT* (*ot907*) and *cho-1/CHT* (*otIs534*) cholinergic reporter expression is not observed in AIM in control animals at the L3 stage (dotted circles, top panels). *lin-28(lf)* and *lin-41(lf)* mutant males show precocious cholinergic gene expression in AIM at the L3 stage (top panels). *eat-4/VGLUT* (*otIs388*) glutamatergic reporter expression is observed in AIM in control animals at the L3 stage (circled in white, bottom panels). *lin-28(lf)* and *lin-41(lf)* mutant males show precocious loss of AIM glutamatergic identity (dotted circles, bottom panels). The AIY cholinergic neuron is located next to AIM and is used as a positional reference.
C: Male-specific AIM differentiation is blocked in *let-7(lf)*, *lin-41(gf) and lin-29(lf)* mutants*. unc-17/VACHT* (*ot907*) and *cho-1/CHT* (*otIs354*) cholinergic reporter expression is observed in young adult (YA) control males but not in AIM neurons in hermaphrodites nor *let-7(lf)*, *lin-41(gf)* and *lin-29(lf)* mutant males (dotted circles, top panels). *eat-4/VGLUT* (*otIs388*) glutamatergic reporter expression is observed in hermaphrodites and in *let-7(lf)*, *lin-41(gf)* and *lin-29(lf)* mutant males, where it fails to be downregulated (circled in white, bottom panels). L1 *let-7(n2853)* animals were shifted to the restrictive temperature (25°C) and imaged after 48hs. The incomplete penetrance of the *let-7* mutants is likely because the allele used, *n2853*, a point mutation in the miRNA seed region, is hypomorphic. The AIY cholinergic neuron is located next to AIM and is used as a positional reference.
D: Quantification for the AIM neurotransmitter switch in heterochronic mutants *lin-28(n719)*, *lin-41(bch28)*, *let-7(n2853)*, *lin-41(xe8)*, *lin-29(n333)* and *mab-10(xe44)* (n=15). Expression of *unc-17/VACHT* (*ot907*) and *eat-4/VGLUT* (*otIs388*) was quantified as ON or OFF.
E: CEM neuronal differentiation defects in heterochronic mutants. CEM cholinergic gene expression is precocious in *lin-28(lf)* and *lin-41(lf)* males compared to control. *unc-17/VACHT* (*ot907*) and *cho-1/CHT* (*otIs354*) cholinergic reporter expression is not observed in CEM neurons in wild type males at the L3 stage (dotted circle). *lin-28(lf)* and *lin-41(lf)* males show precocious cholinergic gene expression in CEM neurons at the L3 stage (circled in white, top panels). CEM cholinergic gene expression is lost in *let-7(lf)* and *lin-41(gf)* mutants (dotted circles). *lin-29(lf)* mutants showed no defect cholinergic gene expression in CEM neurons (circled in white). L1 *let-7(n2853)* animals were shifted to the restrictive temperature (25°C) and imaged after 48hs. The incomplete penetrance of the *let-7* mutants is likely because the allele used, *n2853*, a point mutation in the miRNA seed region, is hypomorphic.
F: Quantification for CEM cholinergic gene expression in heterochronic mutants *lin-28(n719)*, *lin-41(bch28)*, *let-7(n2853)*, *lin-41(xe8)*, *lin-29(n333)* and *mab-10(xe44)* (n=15). Expression of *unc-17/VACHT* (*ot907*) was quantified as ON or OFF.

Figure 2. Temporal expression pattern of endogenously tagged heterochronic pathway effector *lin-29* in the nervous system of both sexes.

A: Cartoon showing the *lin-29* locus. Alternative promoter usage generates two LIN-29 protein isoforms. Exons 1-4 are LIN-29A specific while exons 5-11, that include the Zn-finger DNA binding domain, are shared by both -A and -B isoforms. The *lin-29* locus was tagged using CRISPR/Cas9 genome engineering. *gfp* was inserted either at the C-terminal end (*lin-29a/b::gfp; xe61* allele) to tag both LIN-29A and B protein isoforms or at the N-terminal end (*gfp::lin-29a*; *xe63* allele) to tag only the LIN-29A isoform. Canonical alleles *n333* and *n546* as well as the newly generated alleles *xe37* (null), *xe38* (A-specific) and *xe40* (A-specific) are indicated. Sequence homology alignment of the five Zn-finger domains show that LIN-29 is an orthologue of human ZNF362 and ZNF385, while EGRH-1 is an orthologue of human EGR. The Zn finger of worm, fly and human are shown. Zn coordinating Cys and His residues are colored in blue and DNA-contacting residues (at position -1, +2, +3 and +6 of the helixes preceding the His residues) are colored in red. Conservation is indicated in grey shading.
B: *gfp::lin-29a* expression pattern during larval development in both sexes. Confocal images for endogenously tagged *gfp::lin-29a (xe63)* show that GFP is expressed in male-specific non-neuronal tail cells at the end of the L3 stage and onwards. No expression was observed in the head or tail of the hermaphrodite at this stage. No overlap between GFP and the cholinergic fosmid based reporter *cho-1/CHT* (*otIs544*) was observed at this stage. At the young adult stage, we observed GFP expression in neurons only in males (expression in male neurons started at the L4 stage), indicated by white arrows. No neuronal expression was observed in hermaphrodite neurons. Many GFP positive neurons in the male were also labeled by a cholinergic *cho-1/CHT mCherry* expressing fosmid (*otIs544*). Cholinergic neurons expressing *lin-29a* included AIM, ASJ, AVA and ADF in the head, ventral nerve cord neurons (VNC) corresponding to the A, B and AS classes and PVC in the tail. Neuronal GFP expression is indicated by arrows and neuronal identity is indicated for head and tail neurons in the GFP panels. Ventral nerve cord neurons (VNC) neurons correspond to the A, B, D and AS classes. GFP expression was observed throughout the hypodermis in both sexes, indicated with blue circles in the GFP panels. Hypodermis nuclei are large and more external than neuronal nuclei. In the male, a few neuron classes are labeled in the head and tail. Cholinergic retrovesicular ganglion (RVG), ventral nerve cord (VNC) and pre-anal ganglion (PAG) neurons expressing *lin-29a* are shown in the head, midbody and tail respectively. Hypodermal cell expression is present in both sexes. Scale bar: *10μm*.

Figure 3. Cell-autonomy and sufficiency of *lin-29* for AIM neurotransmitter switch.

A: The neurotransmitter switch is blocked in three newly generated *lin-29* mutants. In adult control animals, the fosmid-based cholinergic reporters *unc-17/VACHT* (*otIs576*) and *cho-1/CHT* (*otIs544*) are expressed in AIM neurons of adult males but not hermaphrodites while the *eat-4/VGLUT* (*otIs518*) glutamatergic reporter is expressed in AIM neurons of adult hermaphrodites but not males. The AIM neurotransmitter switch is blocked in a newly generated *lin-29(xe37)* null allele and in two *lin-29a*-specific mutants (*xe38* and *xe40*). In these *lin-29* mutant males, AIM fails to turn on cholinergic markers *unc-17/VACHT* (top panels) and *cho-1/CHT* (bottom panels) and expresses a pan neuronal maker *rab-3::rfp* (top panels) and the glutamatergic marker *eat-4/VGLUT* (bottom panels). A pan-neuronal *rab-3::rfp* (*otIs355*) reporter was used to label all neurons in the top panels.
B: AIM specific LIN-29A expression is sufficient to cell-autonomously rescue the neurotransmitter switch in males and induce it in young larvae and the opposite sex. LIN-29A expression was driven under an AIM-specific promoter in *lin-29a* mutant animals: LIN-29A was expressed in *lin-29a(xe38)* (*otEx7316* and *otEx7317*) and in *lin-29a(xe40)* (*otEx7318* and *otEx7319*). Expression of cholinergic gene reporter *unc-17/VACHT* (*otIs576*) was examined to assay rescue and ectopic induction of the AIM neurotransmitter switch (n=15).

Figure 4. Male-specific molecular differentiation programs are lost in *lin-29a* mutants.

A: Male-specific expression of *srj-54* in AIM requires *lin-29a*. Expression of the GPCR *srj-54 (fsIs5)* promoter fusion is observed in adult males but not hermaphrodites in the AIM interneurons. Expression of *srj-54* was lost in all the *lin-29a(xe38)* mutant males. Quantification is shown on the right (n=15). Scale bar: *10µm*.
B: Male-specific expression of *dmd-5* in AVG requires *lin-29a*. Expression of the DM-containing transcription factor promoter fusion *dmd-5* (*pUL#JS9B3*) is observed in adult males but not hermaphrodites in the AVG interneuron. In the absence of *lin-29a*, expression is lost from AVG in 80% of the male worms (top panels); quantification is shown on the right (n=15). The expression of the daf-7/*TGFβ*-like molecule promoter fusion is observed in adult males but not hermaphrodites and this expression is lost in the *lin-29a(xe38)* mutant males (bottom panels). Quantification is shown on the right (n=15). Scale bar: *10um*.
C: *lin-29a* is required for normal PDB branching. A reporter fragment from the extracellular cell adhesion molecule *kal-1* is expressed in a number of neurons in the tail region in both sexes, including the PDB –inter and motorneuron (Wenick and Hobert, 2004). *kal-1::gfp* reporter expression showed that the PDB neuron process exhibits elaborate branching in the male after sexual maturation but not at earlier larval stages. In the absence of *lin-29a*, PDB branching is lost from adult males (bottom panels). Quantification of total neurite length is shown on the right (n=10). PDB neurites establish extensive electrical and chemical synapses with sex-shared and male-specific neurons exclusively in adult males (schematized; LIN-29A(+) neurons are shown in blue text)(Jarrell et al., 2012). Scale bar: *5µm*.

Figure 5. *lin-29A* is required for adult male-specific behaviors.

A: *lin-29a* is required for male mating. The ability of the of *lin-29a(xe38)* and *lin-29a(xe40)* mutant males to locate the hermaphrodite vulva is significantly reduced compared to *lin-29(+)* control males (n=15).
B: *lin-29a* is required for male-specific mate searching behavior. Young adult males are followed over time and scored for movement beyond 3cm away from the food source. *lin-29Aa(xe38)* mutant males failed to leave the food and search for mates and behaved similarly to *wild type* hermaphrodites. *lin-29a* mate-searching defect could be partially rescued by restoring LIN-29A expression in AIM interneurons (*otEx7316*). Values plotted are an average of two independent experiments (n=15 for each experiment).
C: *lin-29a* dependent and *lin-29a* independent adult-specific sexually dimorphic locomotory features. Cartoon of an adult *C. elegans* depicts the location of the body parts used for feature computation. The arrows for each body part represent the bend angle. Wavelength and amplitude while crawling are shown. Adult hermaphrodites and males showed sex-specific differences in posture, path and locomotory features that were not affected by *lin-29a* absence (top panel). A complete list of sexually dimorphic features not affected by *lin-29a* is provided in Table S1. In the *lin-29a* mutant males, a number of sexually dimorphic features were feminized compared to *wild type* males (bottom panel), including posture and locomotory features. When LIN-29A was restored to the command interneuron AVA and ventral nerve cord motor neurons (*otEx7320*), it partially rescued the feminization of two postural features (midbody bend and wavelength) as well as one locomotory feature (midbody crawling amplitude) (n=20).

Figure 6. Intersectional control of distinct *lin-41* effectors via heterochronic, sexual (*tra-1*) and spatial (terminal selector) inputs.

A: LIN-29 neuronal expression is regulated by the sex-determination pathway. Mutant hermaphrodites for the downstream effector of the sex-determination pathway *tra-1* showed *lin-29a/b::gfp (xe61)* expression in hermaphrodite neurons in L4 and adult stages. Masculinization of the hermaphrodite nervous system by a pan-neuronal promoter driving *fem-3 (otEx7321),* that represses *tra-1,* induced *lin-29a/b::gfp* (*xe61*) expression in hermaphrodite neurons in L4 and onwards.
B: *lin-29a/b::gfp* neuronal expression is lost in neuron-specific transcription factor mutants. The POU homeobox transcription factor *unc-86* is required for *lin-29a/b::gfp* expression in AIM interneurons. The LIM-HD transcription factor *ttx-3* is required for *lin-29a/b::gfp* expression in ASK. The COE/EBF transcription factor *unc-3* is required for *lin-29a/b::gfp* expression in AVA, SAB, DA, DB, VA, VB, PDA, PDB and PVC neurons. Cholinergic neurons are labeled with the *cho-1/CHT mCherry* fosmid reporter.
C: *mab-3::gfp* expression in the SMD neurons in control hermaphrodites, males and mutant animals. *mab-3::gfp* (*ot931*) expression was determined during larval development. GFP was first observed in the SMD neurons at the L4 stage and onwards, only in males. *mab-3::gfp* expression was lost from SMD neurons in a *let-7(n2853)* mutant male. L1 *let-7(n2853)* animals were shifted to the restricted temperature (25°C) and imaged as adults, after 48hs. *mab-3::gfp* expression was lost from SMD neurons in an *unc-42(e419)* mutant male. Scale bar: *5µm*.
D: *dmd-3::gfp* expression in the PHC neuron in control hermaphrodites, males and mutant animals. *dmd-3::gfp* (*ot932*) expression was determined during larval development. GFP was first observed in the PHC neurons at the L4 stage and onwards, only in males. *dmd-3::gfp* expression was decreased from PHC neurons in a *let-7(n2853)* mutant male. L1 *let-7(n2853)* animals were shifted to the restricted temperature (25°C) and imaged as adults, after 48hs.
E: *dmd-3::gfp* expression was lost from PHC neuron in a *ceh-14* null mutant male. *dmd-3::gfp* (*ot932*) expression was lost from PHC neuron in a *let-7(n2853)* mutant male. L1 *let-7(n2853)* animals were shifted to the restricted temperature (25°C) and imaged as adults, after 48hs.
F: Masculinization of the hermaphrodite nervous system by a pan-neuronal promoter driving *fem-3* (*otEx7322 and otEx7323, respectively*), that promotes TRA-1 degradation, induced *mab-3::gfp (ot931)* expression in hermaphrodite SMD neurons and. *dmd-3::gfp (ot932)* expression in hermaphrodite PHC neurons in L4 and onwards.

Figure 7. Timing mechanisms controlling sexually dimorphic nervous system differentiation during sexual maturation.

A: The evolutionarily conserved *lin-28/let-7/lin-41* heterochronic pathway controls the timing of the expression of multiple neuron-specific effectors in the male nervous system. The RNA-binding protein LIN-28 controls the expression of the miRNA *let-7*, which in turn controls expression of the RNA-binding protein LIN-41. LIN-41 *let-7*-mediated downregulation at the onset of sexual maturation de-represses LIN-41 targets LIN29A, MAB-3 and DMD-3. Expression of these LIN-41 effectors in specific neurons in males, at the onset of sexual maturation, constitute effector modules directing the precisely timed nervous system masculinization. We hypothesize that similar LIN-41 effectors, not identified yet, could be acting in other neurons in the male nervous system and in the hermaphrodite nervous system.
B: Temporal, sex-specific and neuron-specific intersectional control of nervous system differentiation during sexual maturation. A hypothetical male neuron is shown. As discussed above, LIN-41 repression of the heterochronic pathway is relieved at the onset of sexual maturation, allowing neuron-specific effector proteins to be expressed. In males, degradation of the ubiquitously expressed transcriptional repressor TRA-1 allows expression of male-specific regulatory effectors (blue boxes same as panel A). The neuron type-specificity of regulatory effector gene expression is determined by terminal selector transcription factors that control the expression of many other neuronal identity features. Hence, terminal selectors define a neuron type-specific, but permissive state whose sex- and time-specificity is controlled by factors that antagonize the effect of terminal selectors on regulatory effector genes (transcriptionally – TRA; translationally – LIN-41). Note that features that are controlled by sex/time-specific regulatory effectors, exemplified by LIN-29A regulation of neurotransmitter pathway genes, are also controlled by terminal selectors, thereby constituting a “feedforward” regulatory architecture.

SUPPLEMENTARY FIGURES

Figure S1. AIM and CEM neuronal differentiation does not require the gonad nor the germline.

A: Expression pattern for the endogenously tagged *unc-17/VACHT* allele during development. We used CRISPR/Cas9 genome editing to place an *mKate2::3xFLAG* tag on the C-terminal end of the *unc-17/VACHT* locus. The endogenously tagged cholinergic locus (*ot907*) recapitulates our previously described *unc-17/VACHT* expression, assessed with a fosmid-based reporter. The confocal images show that *unc-17/VACHT* is expressed in AIM sex-shared neurons only in the males (bottom panels), but not in hermaphrodites (top panels), starting at the L4 stage. Each image square inset is zoomed in at the top right corner. AIM neurons are circled inside each inset at the different developmental stages. CEM male-specific neurons showed *unc-17/VACHT* expression also starting at the L4 stage (circled at the different larval stages). The *cho-1/CHT* fosmid-based *yfp* reporter (*otIs534*) was used to label the neuronal nuclei of cholinergic neurons facilitating their identification.
B: Germline loss has no effect on AIM nor CEM cholinergic gene expression in males. *glp-1(e2141)* mutants showed no difference in expression of cholinergic genes *unc-17/VACHT* and *cho-1/CHT* in AIM and CEM neurons compared to control adult males. Confocal images for a young adult hermaphrodite (top panel) and young adult male (bottom panel) are shown.
C: Laser ablation of gonad precursors has no effect on AIM and CEM cholinergic gene expression in males. Z1/Z4 gonad and germline precursors were ablated at the L1 stage. No difference was observed in the expression of the cholinergic gene *cho-1/CHT* (*otIs534*) in the AIM and CEM neurons of Z1/Z4 ablated adult male animals compared to control animals. All neurons are labeled with a red pan-neuronal *rab-3* reporter (*otIs355*).

Figure S2: Temporal expression pattern of heterochronic pathway genes *mab-10, lin-28, lin-41 and let-7* in the nervous system.

A: *mab-10::mCherry* expression pattern during larval development in both sexes. An endogenously tagged *mab-10* allele (*xe75*) showed ubiquitous expression starting in the L4 stage, including in the nervous system. Reporter expression was maintained in the adult. No sexually dimorphic differences were observed for *mab-10* expression. A cartoon for the *mab-10* locus is shown below the images.
B: *lin-28::gfp* expression pattern during early larval development. A *lin-28::gfp* fosmid-based reporter (*wgIs535*) showed ubiquitous expression at the L2 stage, including in the nervous system. Reporter expression was broadly downregulated at the L3 and L4 stages. The fosmid-based *cho-1/CHT* reporter (*otIs544*) was used to label cholinergic neurons. No sexually dimorphic differences were observed for *lin-28* expression.
C: *lin-41* expression pattern during larval development in both sexes. An endogenously tagged *lin-41* allele (*tn1541*) showed ubiquitous expression at the L3 stage, including in the nervous system. Reporter expression is broadly downregulated at the L4 stage. Expression of *lin-41::gfp* was maintained in two neuronal pairs in the head (black arrows). No sexually dimorphic differences were observed for *lin-41* expression. A cartoon for the *lin-41* locus is shown below the images.
D: *let-7* activity sensor and control sensor expression during larval development in both sexes. A *lin-41* promoter fusion driving *gfp* and fused to the *lin-41* 3'UTR (*xeSi182*), which is directly targeted by *let-7* miRNA, showed ubiquitous expression of *gfp* in the nervous system from the L1 to the L3 stage. At the L4 stage, reporter expression is broadly downregulated and only a few cells are labeled by GFP in the adult head, recapitulating the *lin-41::gfp* expression. The same *lin-41* promoter fusion driving *gfp* and fused to the *unc-54* 3' UTR (*xeSi202*) failed to be normally downregulated at the L4 stage showing that *lin-41* downregulation requires its 3'UTR being bound by miRNA *let-7*. Cholinergic neurons were labeled by a *cho-1/CHT* fosmid reporter (*otIs544*) driving *mCherry* allowing us to correlate the *lin-41* downregulation with AIM neurotransmitter switch in males at the L4 stage. No sexually dimorphic differences in *gfp* expression were observed for the *let-7* sensor and its control. Cartoons for each construct are shown above the images.

Figure S3. Expression pattern for *lin-29* isoforms.

A: *lin-29a/b* expression pattern during larval development in both sexes. Confocal images for endogenously tagged *lin-29a/b::gfp (xe63)* show that GFP is expressed in the pharynx at the L3 stage and onwards in both sexes (examination of young animals showed that pharyngeal expression starts at the L1 stage). Hypodermal GFP expression all along the body started at the end of the L3 stage in both sexes. At the L4 stage we also detected GFP expression in neurons only in the male, many of which were also labeled by a cholinergic *cho-1/CHT mCherry* expressing fosmid (marked by arrows). Expression in these male neurons persisted in the adult stage. No neuronal expression was observed in the head nor tail in hermaphrodite animals. Scale bar: *10um*.
B: *lin-29b* expression pattern at the young adult stage in both sexes. Confocal images for endogenously tagged *lin-29b::gfp; lin-29a(xe40) (xe65)* show that GFP is expressed in head glia in both sexes (marked by arrows). GFP is also observed in the pharynx and in tail cells in both sexes. Cholinergic *cho-1/CHT mCherry* expressing fosmid (*otIs544*) did not co-localize with GFP showing that LIN-29B is not expressed in neurons in the head nor tail in either sex (Note that LIN-29B is expressed in midbody neurons in both sexes not shown in this image). Scale bar: *10um*.

Figure S4. LIN29A neuronal expression is regulated by *lin-41* and *let-7*.

A: *gfp::lin-29a* neuronal expression is precocious in the absence of *lin-41.* Expression of *gfp::lin-29a* (*xe63*) was determined in synchronized L3 animals and compared between *lin-41(n2914)/balancer* control versus *lin-41(n2914) loss of function* males. While the heterozygous control males did not show *gfp::lin-29a* expression at this larval stage in the head, the *lin-41* loss of function males showed precocious *gfp::lin-29a* expression, including in the hypodermis and nervous system. The AIM *gfp::lin-29a* expression is marked with an arrow.
B: *gfp::lin-29a* neuronal expression is downregulated in the *let-7(lf) and lin-41(gf)* mutants. Expression of *gfp::lin-29a* (*xe63*) was determined at the young adult stage in *let-7(n2853*) *loss of function* mutants and *lin-41(xe8) gain of function* mutants*,* compared to control males*.* While control males showed expression of *gfp::lin-29a* in the hypodermis and nervous system, as previously described, both mutants showed a severe downregulation of *gfp::lin-29a* expression in the hypodermis and neurons at the young adult stage. The AIM *gfp::lin-29a* expression is marked with an arrow. L1 *let-7(n2853)* animals were shifted to the restricted temperature (25°C) and imaged as adults, after 48hs.

Figure S5. *lin-29A* mutants show a normal male tail morphology.

A: DIC images for young adult *wild type* and *lin-29a* mutants *xe38* and *xe40*. No morphological defects were detected in the young adult *lin-29a* mutant males compared to *wild type*. 20x images for young adult males are shown on the top panels. 63x images of the male tail are shown on the bottom panels.
B: WormTracker analysis of sexually dimorphic postural features showed no difference between wild type and *lin-29a* mutant males. Hermaphrodites and males were tracked for five minutes and features describing body posture were analyzed using the WormTracker software. Adult hermaphrodites and males showed sex-specific differences in posture including length, head width, midbody width and area. When wild type males were compared to *lin-29a xe38* and *xe40* mutant males no significant differences were found.

Bibliography

Abreu, A.P., Dauber, A., Macedo, D.B., Noel, S.D., Brito, V.N., Gill, J.C., Cukier, P., Thompson, I.R., Navarro, V.M., Gagliardi, P.C.*, et al.* (2013). Central precocious puberty caused by mutations in the imprinted gene MKRN3. N Engl J Med *368*, 2467-2475.

Aeschimann, F., Kumari, P., Bartake, H., Gaidatzis, D., Xu, L., Ciosk, R., and Grosshans, H. (2017). LIN41 Post-transcriptionally Silences mRNAs by Two Distinct and Position-Dependent Mechanisms. Mol Cell *65*, 476-489 e474.

Ambros, V. (1989). A hierarchy of regulatory genes controls a larva-to-adult developmental switch in C. elegans. Cell *57*, 49-57.

Ambros, V., and Horvitz, H.R. (1984). Heterochronic mutants of the nematode Caenorhabditis elegans. Science *226*, 409-416.

Arantes-Oliveira, N., Apfeld, J., Dillin, A., and Kenyon, C. (2002). Regulation of life-span by germ-line stem cells in Caenorhabditis elegans. Science *295*, 502-505.

Avendano, M.S., Vazquez, M.J., and Tena-Sempere, M. (2017). Disentangling puberty: novel neuroendocrine pathways and mechanisms for the control of mammalian puberty. Hum Reprod Update *23*, 737-763.

Barr, M.M., Garcia, L.R., and Portman, D.S. (2018). Sexual Dimorphism and Sex Differences in Caenorhabditis elegans Neuronal Development and Behavior. Genetics *208*, 909-935.

Barrios, A., Ghosh, R., Fang, C., Emmons, S.W., and Barr, M.M. (2012). PDF-1 neuropeptide signaling modulates a neural circuit for mate-searching behavior in C. elegans. Nat Neurosci *15*, 1675-1682.

Bettinger, J.C., Lee, K., and Rougvie, A.E. (1996). Stage-specific accumulation of the terminal differentiation factor LIN- 29 during Caenorhabditis elegans development. Development *122*, 2517-2527.

Bulcao Macedo, D., Nahime Brito, V., and Latronico, A.C. (2014). New causes of central precocious puberty: the role of genetic factors. Neuroendocrinology *100*, 1-8.

Bussing, I., Slack, F.J., and Grosshans, H. (2008). let-7 microRNAs in development, stem cells and cancer. Trends Mol Med *14*, 400-409.

Chen, Y.C., Chen, L.M., Lin, H.H., Chen, B.H., Chao, M.C., and Hsiao, H.P. (2017). Association study of LIN28B in girls with precocious puberty. J Pediatr Endocrinol Metab *30*, 663-667.

Corre, C., Shinoda, G., Zhu, H., Cousminer, D.L., Crossman, C., Bellissimo, C., Goldenberg, A., Daley, G.Q., and Palmert, M.R. (2016). Sex-specific regulation of weight and puberty by the Lin28/let-7 axis. J Endocrinol *228*, 179-191.

Del Rio-Albrechtsen, T., Kiontke, K., Chiou, S.Y., and Fitch, D.H. (2006). Novel gain-of-function alleles demonstrate a role for the heterochronic gene lin-41 in C. elegans male tail tip morphogenesis. Dev Biol *297*, 74-86.

Desai, C., Garriga, G., McIntire, S.L., and Horvitz, H.R. (1988). A genetic pathway for the development of the Caenorhabditis elegans HSN motor neurons. Nature *336*, 638-646.

Dickinson, D.J., Pani, A.M., Heppert, J.K., Higgins, C.D., and Goldstein, B. (2015). Streamlined Genome Engineering with a Self-Excising Drug Selection Cassette. Genetics *200*, 1035-1049.

Ecsedi, M., and Grosshans, H. (2013). LIN-41/TRIM71: emancipation of a miRNA target. Genes Dev *27*, 581-589.

Ecsedi, M., Rausch, M., and Grosshans, H. (2015). The let-7 microRNA directs vulval development through a single target. Dev Cell *32*, 335-344.

Emmons, S.W. (2018). Neural Circuits of Sexual Behavior in Caenorhabditis elegans. Annu Rev Neurosci *41*, 349-369.

Euling, S., and Ambros, V. (1996). Heterochronic genes control cell cycle progress and developmental competence of C. elegans vulva precursor cells. Cell *84*, 667-676.
Euling, S., Bettinger, J.C., and Rougvie, A.E. (1999). The LIN-29 transcription factor is required for proper morphogenesis of the Caenorhabditis elegans male tail. Dev Biol *206*, 142-156.
Faunes, F., and Larrain, J. (2016). Conservation in the involvement of heterochronic genes and hormones during developmental transitions. Dev Biol *416*, 3-17.
Fujiwara, M., Aoyama, I., Hino, T., Teramoto, T., and Ishihara, T. (2016). Gonadal Maturation Changes Chemotaxis Behavior and Neural Processing in the Olfactory Circuit of Caenorhabditis elegans. Curr Biol *26*, 1522-1531.
Gonzalez-Itier, S., Contreras, E.G., Larrain, J., Glavic, A., and Faunes, F. (2018). A role for Lin-28 in growth and metamorphosis in Drosophila melanogaster. Mech Dev.
Grosshans, H., Johnson, T., Reinert, K.L., Gerstein, M., and Slack, F.J. (2005). The temporal patterning microRNA let-7 regulates several transcription factors at the larval to adult transition in C. elegans. Dev Cell *8*, 321-330.
Hallam, S.J., and Jin, Y. (1998). lin-14 regulates the timing of synaptic remodelling in Caenorhabditis elegans. Nature *395*, 78-82.
Harris, D.T., and Horvitz, H.R. (2011). MAB-10/NAB acts with LIN-29/EGR to regulate terminal differentiation and the transition from larva to adult in C. elegans. Development *138*, 4051-4062.
He, C., Kraft, P., Chen, C., Buring, J.E., Pare, G., Hankinson, S.E., Chanock, S.J., Ridker, P.M., Hunter, D.J., and Chasman, D.I. (2009). Genome-wide association studies identify loci associated with age at menarche and age at natural menopause. Nat Genet *41*, 724-728.
Herrera, R.A., Kiontke, K., and Fitch, D.H. (2016). Makorin ortholog LEP-2 regulates LIN-28 stability to promote the juvenile-to-adult transition in Caenorhabditis elegans. Development *143*, 799-809.
Hilbert, Z.A., and Kim, D.H. (2017). Sexually dimorphic control of gene expression in sensory neurons regulates decision-making behavior in C. elegans. eLife *6*.
Hobert, O. (2016). Terminal Selectors of Neuronal Identity. Curr Top Dev Biol *116*, 455-475.
Howell, K., White, J.G., and Hobert, O. (2015). Spatiotemporal control of a novel synaptic organizer molecule. Nature *523*, 83-87.
Hsin, H., and Kenyon, C. (1999). Signals from the reproductive system regulate the lifespan of C. elegans. Nature *399*, 362-366.
Jarrell, T.A., Wang, Y., Bloniarz, A.E., Brittin, C.A., Xu, M., Thomson, J.N., Albertson, D.G., Hall, D.H., and Emmons, S.W. (2012). The connectome of a decision-making neural network. Science *337*, 437-444.
Jazin, E., and Cahill, L. (2010). Sex differences in molecular neuroscience: from fruit flies to humans. Nat Rev Neurosci *11*, 9-17.
Juraska, J.M., and Willing, J. (2017). Pubertal onset as a critical transition for neural development and cognition. Brain Res *1654*, 87-94.
Katic, I., Xu, L., and Ciosk, R. (2015). CRISPR/Cas9 Genome Editing in Caenorhabditis elegans: Evaluation of Templates for Homology-Mediated Repair and Knock-Ins by Homology-Independent DNA Repair. G3 (Bethesda) *5*, 1649-1656.
Kim, W., Underwood, R.S., Greenwald, I., and Shaye, D.D. (2018). OrthoList 2: A New Comparative Genomic Analysis of Human and Caenorhabditis elegans Genes. Genetics.
Kleemann, G., Jia, L., and Emmons, S.W. (2008). Regulation of Caenorhabditis elegans male mate searching behavior by the nuclear receptor DAF-12. Genetics *180*, 2111-2122.

Kratsios, P., Stolfi, A., Levine, M., and Hobert, O. (2011). Coordinated regulation of cholinergic motor neuron traits through a conserved terminal selector gene. Nat Neurosci *15*, 205-214.
Lee, G., Foss, M., Goodwin, S.F., Carlo, T., Taylor, B.J., and Hall, J.C. (2000). Spatial, temporal, and sexually dimorphic expression patterns of the fruitless gene in the Drosophila central nervous system. J Neurobiol *43*, 404-426.
Lehrbach, N.J., Armisen, J., Lightfoot, H.L., Murfitt, K.J., Bugaut, A., Balasubramanian, S., and Miska, E.A. (2009). LIN-28 and the poly(U) polymerase PUP-2 regulate let-7 microRNA processing in Caenorhabditis elegans. Nat Struct Mol Biol *16*, 1016-1020.
Lipton, J., Kleemann, G., Ghosh, R., Lints, R., and Emmons, S.W. (2004). Mate searching in Caenorhabditis elegans: a genetic model for sex drive in a simple invertebrate. J Neurosci *24*, 7427-7434.
Liu, K.S., and Sternberg, P.W. (1995). Sensory regulation of male mating behavior in Caenorhabditis elegans. Neuron *14*, 79-89.
Mason, D.A., Rabinowitz, J.S., and Portman, D.S. (2008). dmd-3, a doublesex-related gene regulated by tra-1, governs sex-specific morphogenesis in C. elegans. Development *135*, 2373-2382.
McCarthy, M.M., and Arnold, A.P. (2011). Reframing sexual differentiation of the brain. Nat Neurosci *14*, 677-683.
Moss, E.G., Lee, R.C., and Ambros, V. (1997). The cold shock domain protein LIN-28 controls developmental timing in C. elegans and is regulated by the lin-4 RNA. Cell *88*, 637-646.
Moss, E.G., and Romer-Seibert, J. (2014). Cell-intrinsic timing in animal development. Wiley interdisciplinary reviews Developmental biology *3*, 365-377.
Mowrey, W.R., Bennett, J.R., and Portman, D.S. (2014). Distributed effects of biological sex define sex-typical motor behavior in Caenorhabditis elegans. J Neurosci *34*, 1579-1591.
Olsson-Carter, K., and Slack, F.J. (2010). A developmental timing switch promotes axon outgrowth independent of known guidance receptors. PLoS Genet *6*.
Ong, K.K., Elks, C.E., Li, S., Zhao, J.H., Luan, J., Andersen, L.B., Bingham, S.A., Brage, S., Smith, G.D., Ekelund, U.*, et al.* (2009). Genetic variation in LIN28B is associated with the timing of puberty. Nat Genet *41*, 729-733.
Oren-Suissa, M., Bayer, E.A., and Hobert, O. (2016). Sex-specific pruning of neuronal synapses in Caenorhabditis elegans. Nature *533*, 206-211.
Pereira, L., Kratsios, P., Serrano-Saiz, E., Sheftel, H., Mayo, A.E., Hall, D.H., White, J.G., LeBoeuf, B., Garcia, L.R., Alon, U.*, et al.* (2015). A cellular and regulatory map of the cholinergic nervous system of C. elegans. eLife *4*.
Perry, J.R., Stolk, L., Franceschini, N., Lunetta, K.L., Zhai, G., McArdle, P.F., Smith, A.V., Aspelund, T., Bandinelli, S., Boerwinkle, E.*, et al.* (2009). Meta-analysis of genome-wide association data identifies two loci influencing age at menarche. Nat Genet *41*, 648-650.
Portman, D.S. (2007). Genetic control of sex differences in C. elegans neurobiology and behavior. Adv Genet *59*, 1-37.
Portman, D.S. (2017). Sexual modulation of sex-shared neurons and circuits in Caenorhabditis elegans. J Neurosci Res *95*, 527-538.
Reinhart, B.J., Slack, F.J., Basson, M., Pasquinelli, A.E., Bettinger, J.C., Rougvie, A.E., Horvitz, H.R., and Ruvkun, G. (2000). The 21-nucleotide let-7 RNA regulates developmental timing in Caenorhabditis elegans. Nature *403*, 901-906.
Rougvie, A.E. (2001). Control of developmental timing in animals. Nat Rev Genet *2*, 690-701.

Rougvie, A.E., and Ambros, V. (1995). The heterochronic gene lin-29 encodes a zinc finger protein that controls a terminal differentiation event in Caenorhabditis elegans. Development *121*, 2491-2500.
Ryan, D.A., Miller, R.M., Lee, K., Neal, S.J., Fagan, K.A., Sengupta, P., and Portman, D.S. (2014). Sex, age, and hunger regulate behavioral prioritization through dynamic modulation of chemoreceptor expression. Curr Biol *24*, 2509-2517.
Sangiao-Alvarellos, S., Manfredi-Lozano, M., Ruiz-Pino, F., Navarro, V.M., Sanchez-Garrido, M.A., Leon, S., Dieguez, C., Cordido, F., Matagne, V., Dissen, G.A.*, et al.* (2013). Changes in hypothalamic expression of the Lin28/let-7 system and related microRNAs during postnatal maturation and after experimental manipulations of puberty. Endocrinology *154*, 942-955.
Schulman, B.R., Esquela-Kerscher, A., and Slack, F.J. (2005). Reciprocal expression of lin-41 and the microRNAs let-7 and mir-125 during mouse embryogenesis. Dev Dyn *234*, 1046-1054.
Sempere, L.F., Sokol, N.S., Dubrovsky, E.B., Berger, E.M., and Ambros, V. (2003). Temporal regulation of microRNA expression in Drosophila melanogaster mediated by hormonal signals and broad-Complex gene activity. Dev Biol *259*, 9-18.
Serrano-Saiz, E., Oren-Suissa, M., Bayer, E.A., and Hobert, O. (2017a). Sexually Dimorphic Differentiation of a C. elegans Hub Neuron Is Cell Autonomously Controlled by a Conserved Transcription Factor. Curr Biol *27*, 199-209.
Serrano-Saiz, E., Pereira, L., Gendrel, M., Aghayeva, U., Battacharya, A., Howell, K., Garcia, L.R., and Hobert, O. (2017b). A Neurotransmitter Atlas of the Caenorhabditis elegans Male Nervous System Reveals Sexually Dimorphic Neurotransmitter Usage. Genetics *206*, 1251-1269.
Serrano-Saiz, E., Poole, R.J., Felton, T., Zhang, F., de la Cruz, E.D., and Hobert, O. (2013). Modular Control of Glutamatergic Neuronal Identity in C. elegans by Distinct Homeodomain Proteins. Cell *155*, 659-673.
Sisk, C.L., and Foster, D.L. (2004). The neural basis of puberty and adolescence. Nat Neurosci *7*, 1040-1047.
Slack, F., and Ruvkun, G. (1997). Temporal pattern formation by heterochronic genes. Annu Rev Genet *31*, 611-634.
Slack, F.J., Basson, M., Liu, Z., Ambros, V., Horvitz, H.R., and Ruvkun, G. (2000). The lin-41 RBCC gene acts in the C. elegans heterochronic pathway between the let-7 regulatory RNA and the LIN-29 transcription factor. Mol Cell *5*, 659-669.
Spike, C.A., Coetzee, D., Eichten, C., Wang, X., Hansen, D., and Greenstein, D. (2014). The TRIM-NHL protein LIN-41 and the OMA RNA-binding proteins antagonistically control the prophase-to-metaphase transition and growth of Caenorhabditis elegans oocytes. Genetics *198*, 1535-1558.
Starostina, N.G., Lim, J.M., Schvarzstein, M., Wells, L., Spence, A.M., and Kipreos, E.T. (2007). A CUL-2 ubiquitin ligase containing three FEM proteins degrades TRA-1 to regulate C. elegans sex determination. Dev Cell *13*, 127-139.
Sulem, P., Gudbjartsson, D.F., Rafnar, T., Holm, H., Olafsdottir, E.J., Olafsdottir, G.H., Jonsson, T., Alexandersen, P., Feenstra, B., Boyd, H.A.*, et al.* (2009). Genome-wide association study identifies sequence variants on 6q21 associated with age at menarche. Nat Genet *41*, 734-738.
Sulston, J.E., Albertson, D.G., and Thomson, J.N. (1980). The Caenorhabditis elegans male: postembryonic development of nongonadal structures. Dev Biol *78*, 542-576.
Sulston, J.E., and Horvitz, H.R. (1977). Post-embryonic cell lineages of the nematode, Caenorhabditis elegans. Dev Biol *56*, 110-156.

Sulston, J.E., Schierenberg, E., White, J.G., and Thomson, J.N. (1983). The embryonic cell lineage of the nematode Caenorhabditis elegans. Dev Biol *100*, 64-119.
Von Stetina, S.E., Treinin, M., and Miller, D.M. (2006). The Motor Circuit. Int Rev Neurobiol *69*, 125-167.
Wang, J., Al-Ouran, R., Hu, Y., Kim, S.Y., Wan, Y.W., Wangler, M.F., Yamamoto, S., Chao, H.T., Comjean, A., Mohr, S.E.*, et al.* (2017). MARRVEL: Integration of Human and Model Organism Genetic Resources to Facilitate Functional Annotation of the Human Genome. Am J Hum Genet *100*, 843-853.
Wenick, A.S., and Hobert, O. (2004). Genomic cis-Regulatory Architecture and trans-Acting Regulators of a Single Interneuron-Specific Gene Battery in C. elegans. Dev Cell *6*, 757-770.
White, J.G., Southgate, E., Thomson, J.N., and Brenner, S. (1986). The structure of the nervous system of the nematode *Caenorhabditis elegans*. Philosophical Transactions of the Royal Society of London B Biological Sciences *314*, 1-340.
White, J.Q., Nicholas, T.J., Gritton, J., Truong, L., Davidson, E.R., and Jorgensen, E.M. (2007). The sensory circuitry for sexual attraction in C. elegans males. Curr Biol *17*, 1847-1857.
Wu, Y.C., Chen, C.H., Mercer, A., and Sokol, N.S. (2012). Let-7-complex microRNAs regulate the temporal identity of Drosophila mushroom body neurons via chinmo. Dev Cell *23*, 202-209.
Yang, C.F., and Shah, N.M. (2014). Representing sex in the brain, one module at a time. Neuron *82*, 261-278.
Yemini, E., Jucikas, T., Grundy, L.J., Brown, A.E., and Schafer, W.R. (2013). A database of Caenorhabditis elegans behavioral phenotypes. Nat Methods *10*, 877-879.
Yi, W., Ross, J.M., and Zarkower, D. (2000). Mab-3 is a direct tra-1 target gene regulating diverse aspects of C. elegans male sexual development and behavior. Development *127*, 4469-4480.
Yi, W., and Zarkower, D. (1999). Similarity of DNA binding and transcriptional regulation by Caenorhabditis elegans MAB-3 and Drosophila melanogaster DSX suggests conservation of sex determining mechanisms. Development *126*, 873-881.
Zhu, H., Shah, S., Shyh-Chang, N., Shinoda, G., Einhorn, W.S., Viswanathan, S.R., Takeuchi, A., Grasemann, C., Rinn, J.L., Lopez, M.F.*, et al.* (2010). Lin28a transgenic mice manifest size and puberty phenotypes identified in human genetic association studies. Nat Genet *42*, 626-630.
Zou, Y., Chiu, H., Zinovyeva, A., Ambros, V., Chuang, C.F., and Chang, C. (2013). Developmental decline in neuronal regeneration by the progressive change of two intrinsic timers. Science *340*, 372-376.

Figure 1

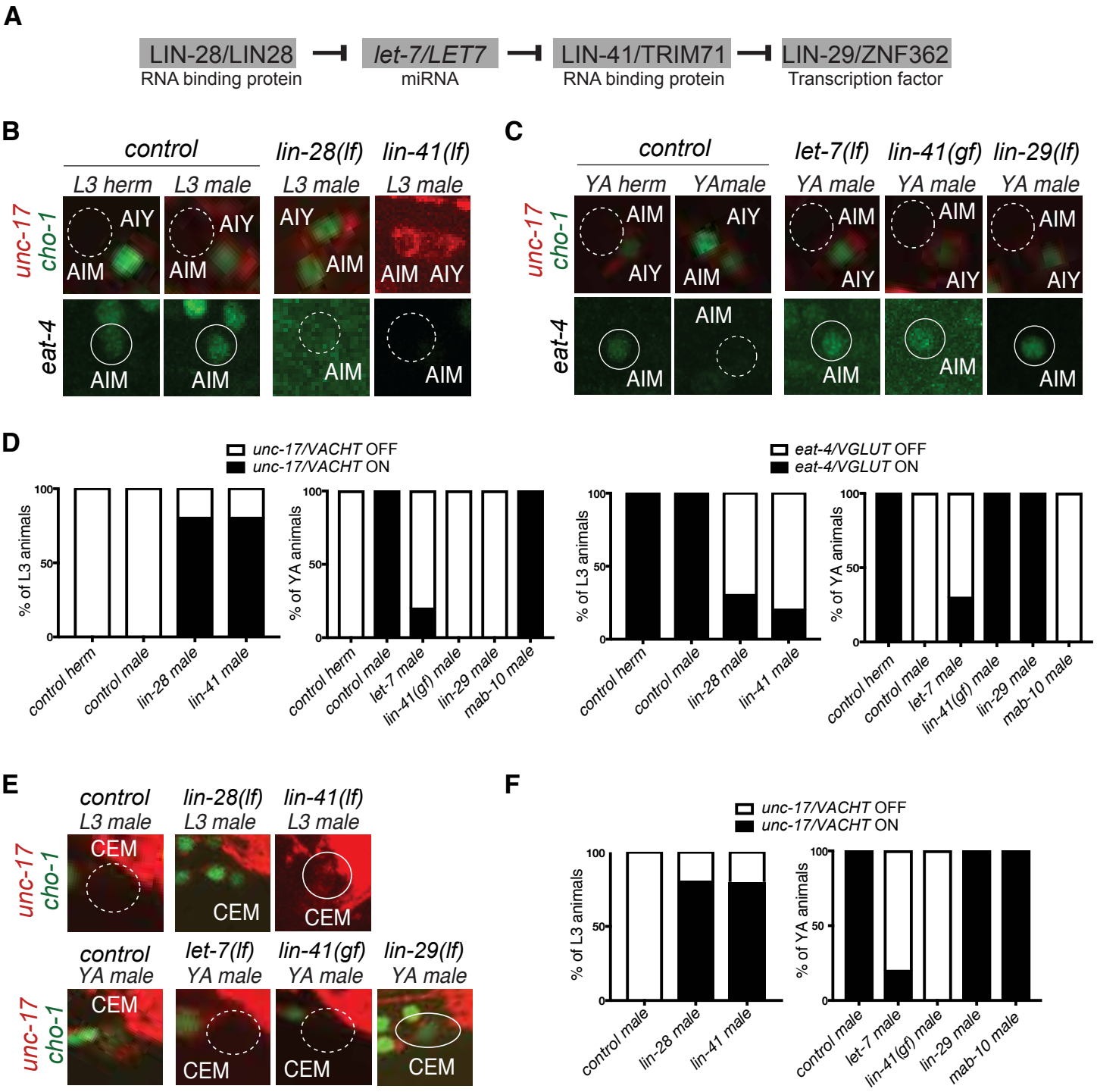
A
LIN-28/LIN28
RNA binding protein
let-7/LET7
miRNA
LIN-41/TRIM71
RNA binding protein
LIN-29/ZNF362
Transcription factor
B
control
lin-28(lf)
lin-41(lf)
L3 herm
L3 male
L3 male
L3 male
unc-17
cho-1
eat-4
AIY
AIM
C
control
let-7(lf)
lin-41(gf)
lin-29(lf)
YA herm
YAmale
YA male
YA male
YA male
D
unc-17/VACHT OFF
unc-17/VACHT ON
eat-4/VGLUT OFF
eat-4/VGLUT ON
% of L3 animals
% of YA animals
100
50
0
control herm
control male
lin-28 male
lin-41 male
let-7 male
lin-41(gf) male
lin-29 male
mab-10 male
E
CEM
F

Figure 2

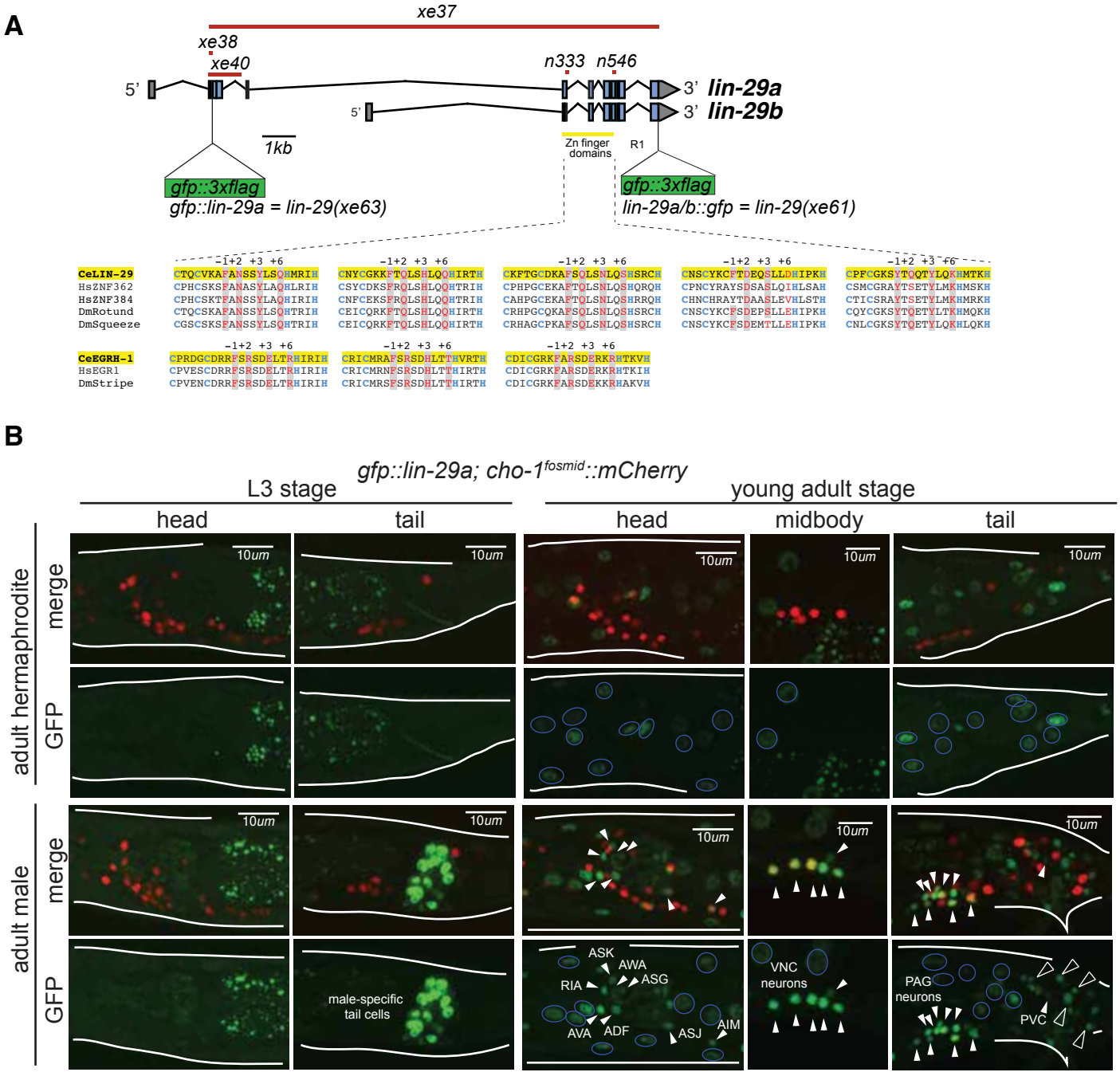
A
xe37
xe38
xe40
n333
n546
5'
5'
3'
3'
lin-29a
lin-29b
1kb
Zn finger domains
R1
gfp::3xflag
gfp::lin-29a = lin-29(xe63)
gfp::3xflag
lin-29a/b::gfp = lin-29(xe61)
-1+2 +3 +6
CeLIN-29 CTQCVKAFANSSYLSQHMRIH CNYCGKKFTQLSHLQQHIRTH CKFTGCDKAFSQLSNLQSHSRCH CNSCYKCFTDEQSLLDHIPKH CPFCGKSYTQQTYLQKHMTKH
HsZNF362 CPHCSKSFANASYLAQHLRIH CSYCDKSFRQLSHLQQHTRIH CPHPGCEKAFTQLSNLQSHQRQH CPNCYRAYSDSASLQIHLSAH CSMCGRAYTSETYLMKHMSKH
HsZNF384 CPHCSKTFANSSYLAQHIRIH CNFCEKSFRQLSHLQQHTRIH CAHPGCEKAFTQLSNLQSHRRQH CHNCHRAYTDAASLEVHLSTH CTICSRAYTSETYLMKHMRKH
DmRotund CTQCSKAFANSSYLSQHTRIH CEICQRKFTQLSHLQQHIRTH CRHPGCQKAFSQLSNLQSHSRCH CNSCYKCFSDEPSLLEHIPKH CQYCGKSYTQETYLTKHMQKH
DmSqueeze CGSCSKSFANSSYLSQHTRIH CEICQRKFTQLSHLQQHIRTH CRHAGCPKAFSQLSNLQSHSRCH CNSCYKCFSDEMTLLEHIPKH CNLCGKSYTQETYLQKHLQKH
CeEGRH-1 CPRDGCDRRFSRSDELTRHIRIH CRICMRAFSRSDHLTTHVRTH CDICGRKFARSDERKRHTKVH
HsEGR1 CPVESCDRRFSRSDELTRHIRIH CRICMRNFSRSDHLTTHIRTH CDICGRKFARSDERKRHTKIH
DmStripe CPVENCDRRFSRSDELTRHIRIH CRICMRSFSRSDHLTTHIRTH CDICGRKFARSDEKKRHAKVH
B
gfp::lin-29a; cho-1fosmid::mCherry
L3 stage
young adult stage
head
tail
head
midbody
tail
adult hermaphrodite
merge
GFP
adult male
merge
GFP
10um
male-specific tail cells
ASK
AWA
ASG
RIA
AVA
ADF
ASJ
AIM
VNC neurons
PAG neurons
PVC

Figure 3

A

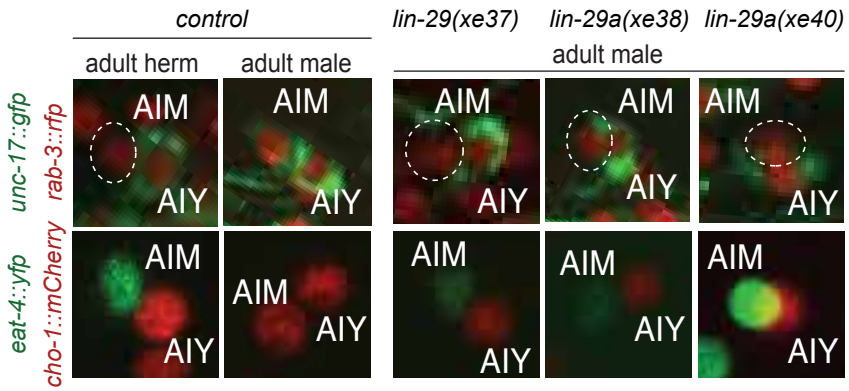
control
lin-29(xe37)
lin-29a(xe38)
lin-29a(xe40)
adult herm
adult male
adult male
unc-17::gfp
rab-3::rfp
eat-4::yfp
cho-1::mCherry
AIM
AIY

B

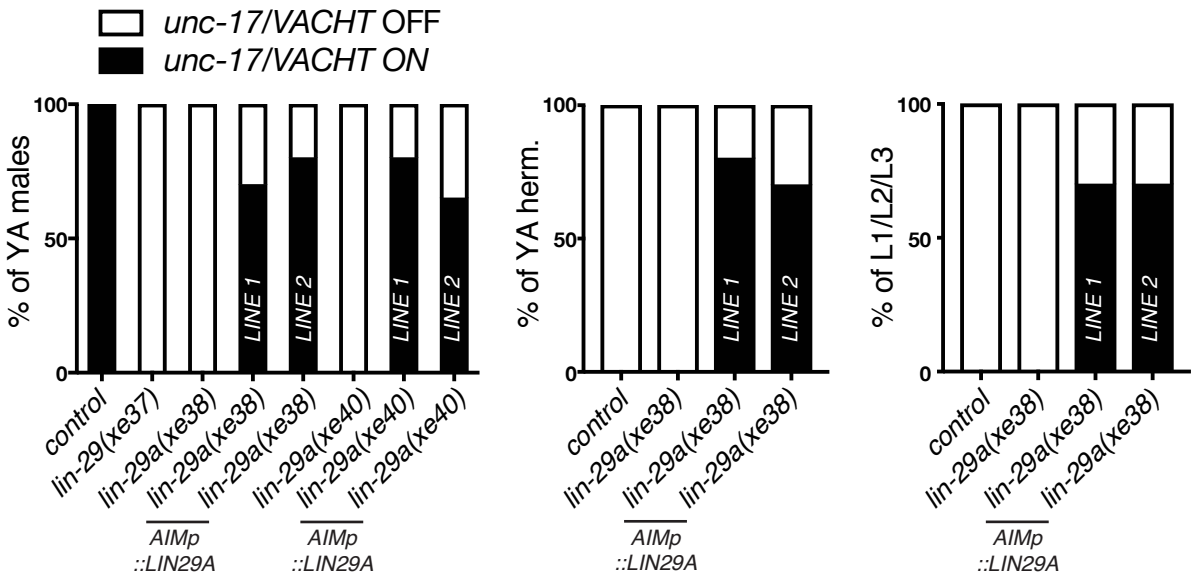
unc-17/VACHT OFF
unc-17/VACHT ON
% of YA males
% of YA herm.
% of L1/L2/L3
100
50
0
LINE 1
LINE 2
control
lin-29(xe37)
lin-29a(xe38)
lin-29a(xe40)
AIMp ::LIN29A

Figure 4

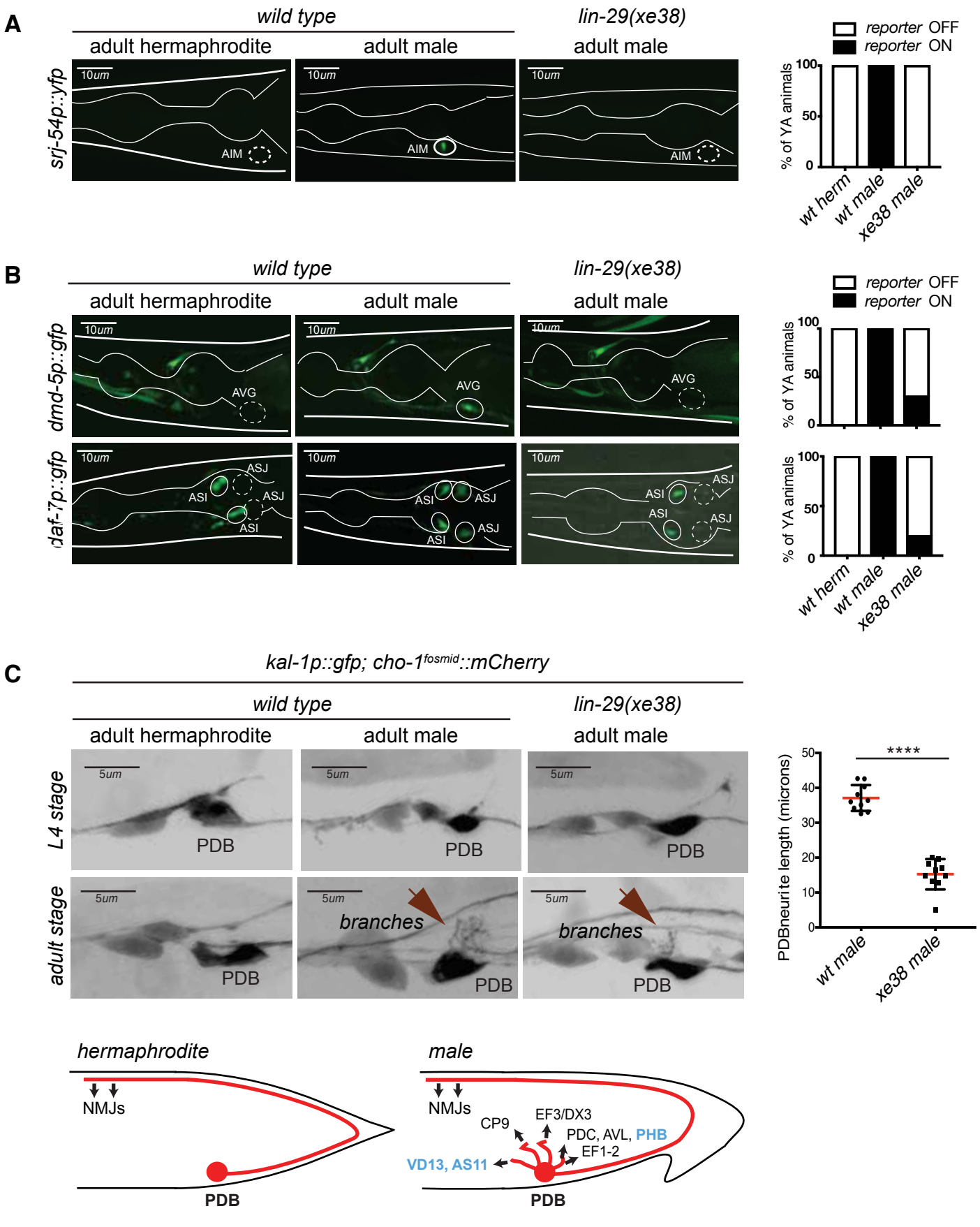
A
wild type
lin-29(xe38)
adult hermaphrodite
adult male
adult male
srj-54p::yfp
10um
AIM
reporter OFF
reporter ON
% of YA animals
100
50
0
wt herm
wt male
xe38 male
B
wild type
lin-29(xe38)
adult hermaphrodite
adult male
adult male
dmd-5p::gfp
daf-7p::gfp
AVG
ASI
ASJ
C
kal-1p::gfp; cho-1fosmid::mCherry
wild type
lin-29(xe38)
adult hermaphrodite
adult male
adult male
L4 stage
adult stage
5um
PDB
branches
PDBneurite length (microns)
****
hermaphrodite
male
NMJs
CP9
EF3/DX3
PDC, AVL, PHB
EF1-2
VD13, AS11

Figure 5

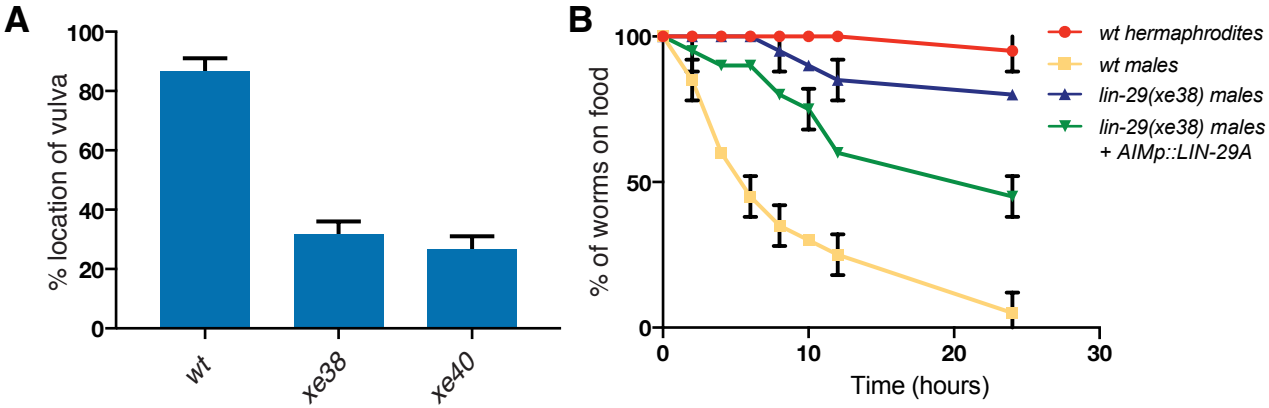
A
% location of vulva
100
80
60
40
20
0
wt
xe38
xe40
B
% of worms on food
100
50
0
0
10
20
30
Time (hours)
wt hermaphrodites
wt males
lin-29(xe38) males
lin-29(xe38) males
+ AIMp::LIN-29A

C

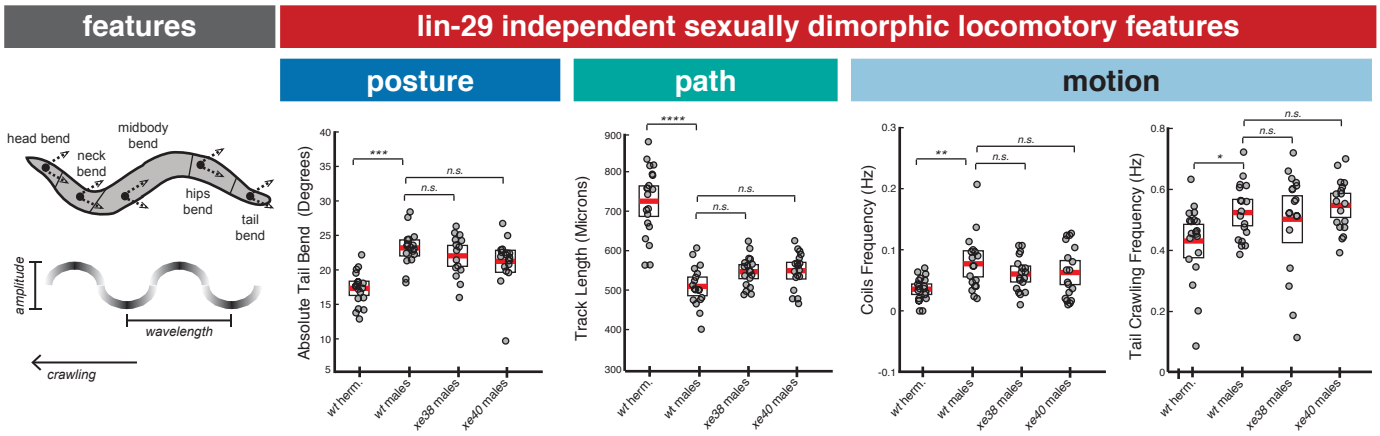
features
lin-29 independent sexually dimorphic locomotory features
posture
path
motion
head bend
neck bend
midbody bend
hips bend
tail bend
amplitude
wavelength
crawling
Absolute Tail Bend (Degrees)
Track Length (Microns)
Coils Frequency (Hz)
Tail Crawling Frequency (Hz)
wt herm.
wt males
xe38 males
xe40 males
n.s.

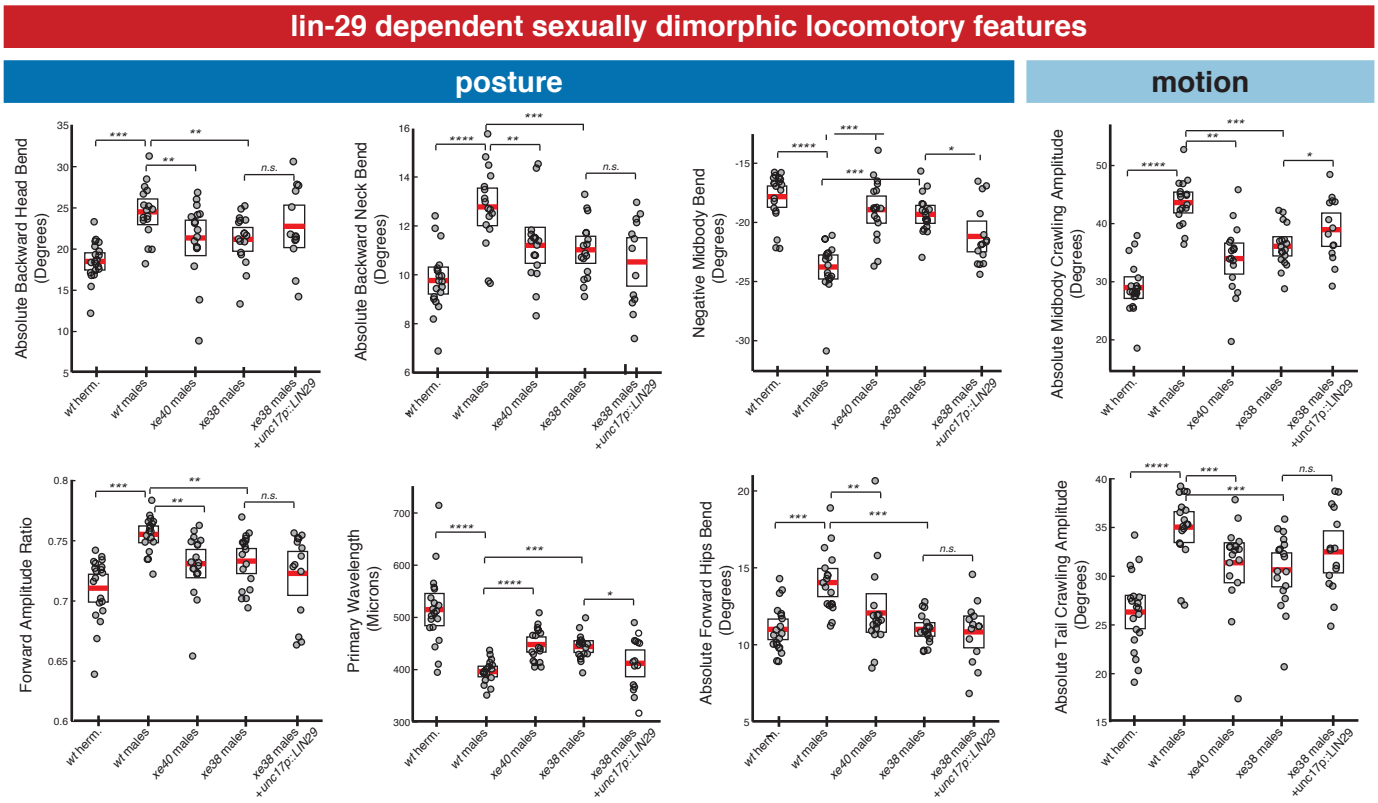
lin-29 dependent sexually dimorphic locomotory features
posture
motion
Absolute Backward Head Bend (Degrees)
Absolute Backward Neck Bend (Degrees)
Negative Midbody Bend (Degrees)
Absolute Midbody Crawling Amplitude (Degrees)
Forward Amplitude Ratio
Primary Wavelength (Microns)
Absolute Forward Hips Bend (Degrees)
Absolute Tail Crawling Amplitude (Degrees)
wt herm.
wt males
xe40 males
xe38 males
xe38 males +unc17p::LIN29
n.s.

Figure 6

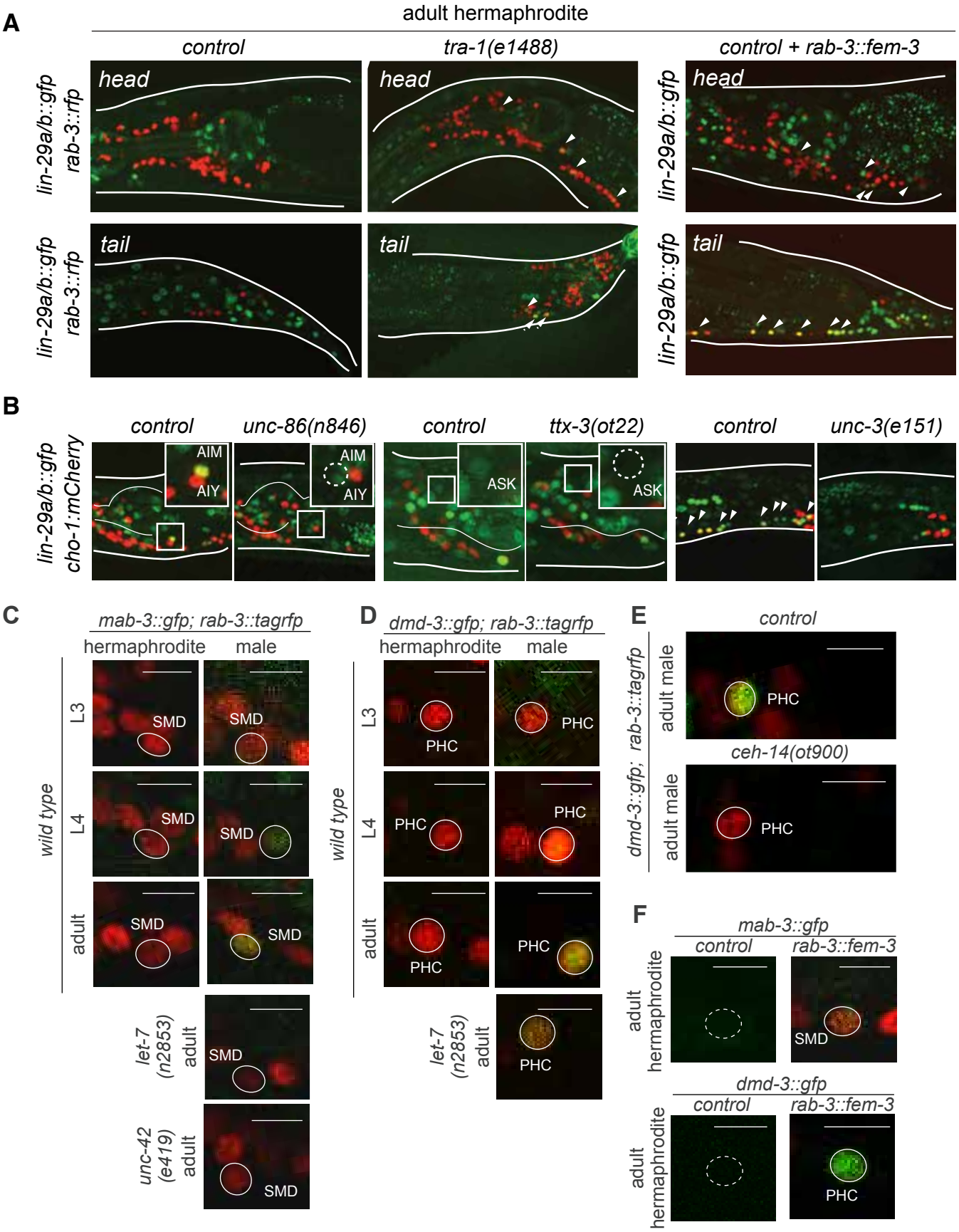
A
adult hermaphrodite
control
tra-1(e1488)
control + rab-3::fem-3
lin-29a/b::gfp
rab-3::rfp
head
tail
B
control
unc-86(n846)
ttx-3(ot22)
unc-3(e151)
lin-29a/b::gfp
cho-1:mCherry
AIM
AIY
ASK
C
mab-3::gfp; rab-3::tagrfp
hermaphrodite
male
wild type
L3
L4
adult
SMD
let-7 (n2853) adult
unc-42 (e419) adult
D
dmd-3::gfp; rab-3::tagrfp
PHC
E
control
dmd-3::gfp; rab-3::tagrfp
adult male
ceh-14(ot900)
F
mab-3::gfp
control
rab-3::fem-3
adult hermaphrodite
dmd-3::gfp

A

Neuron type-specific and sex-specific
modular outputs of heterochronic pathway

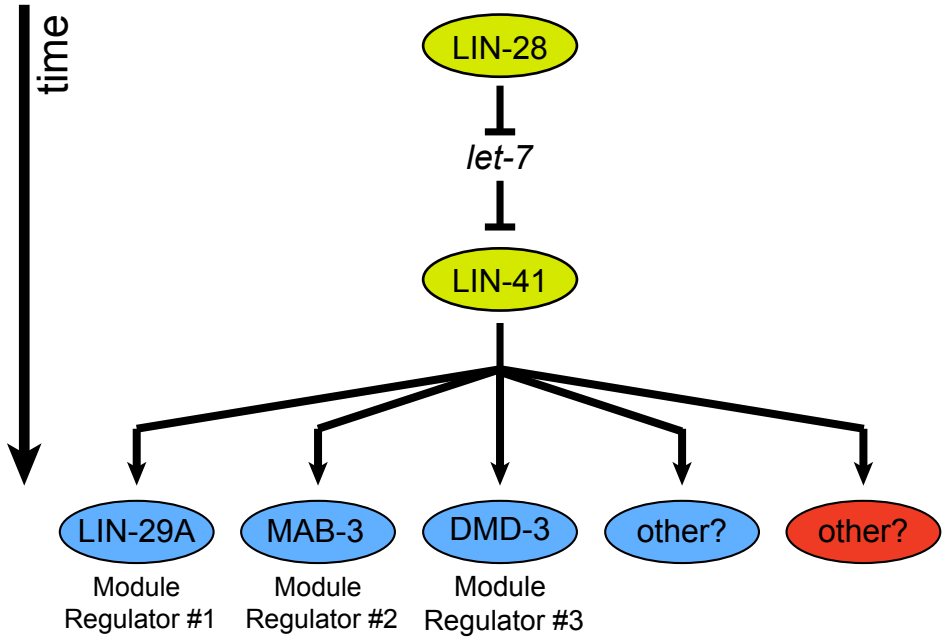

B

Sexually dimorphic male neuron

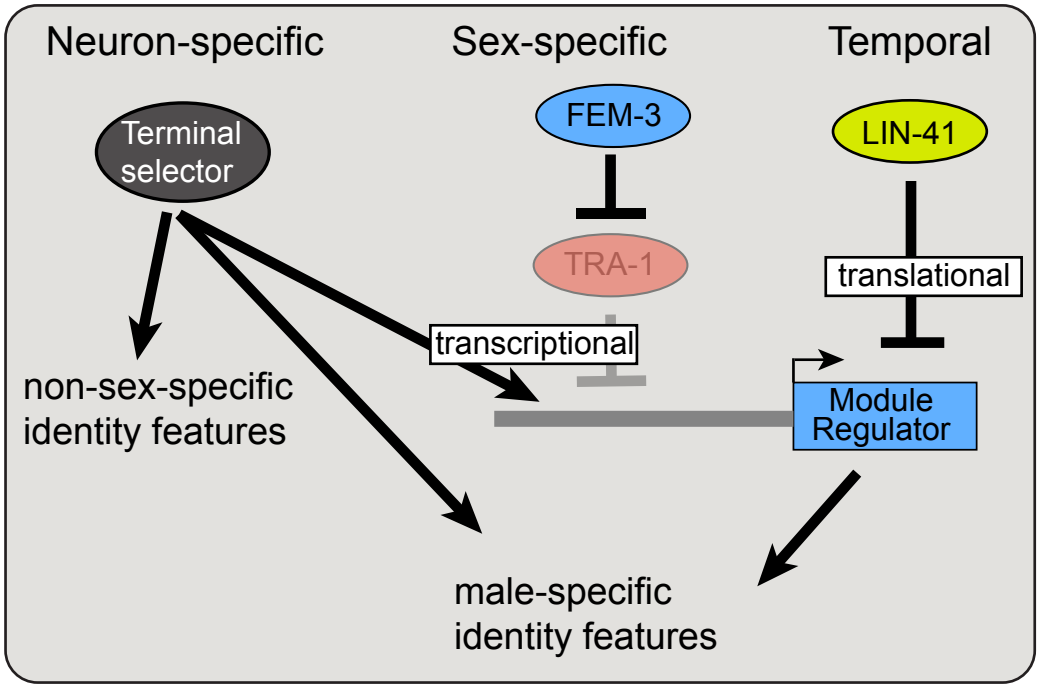

Supplementary Figure 1

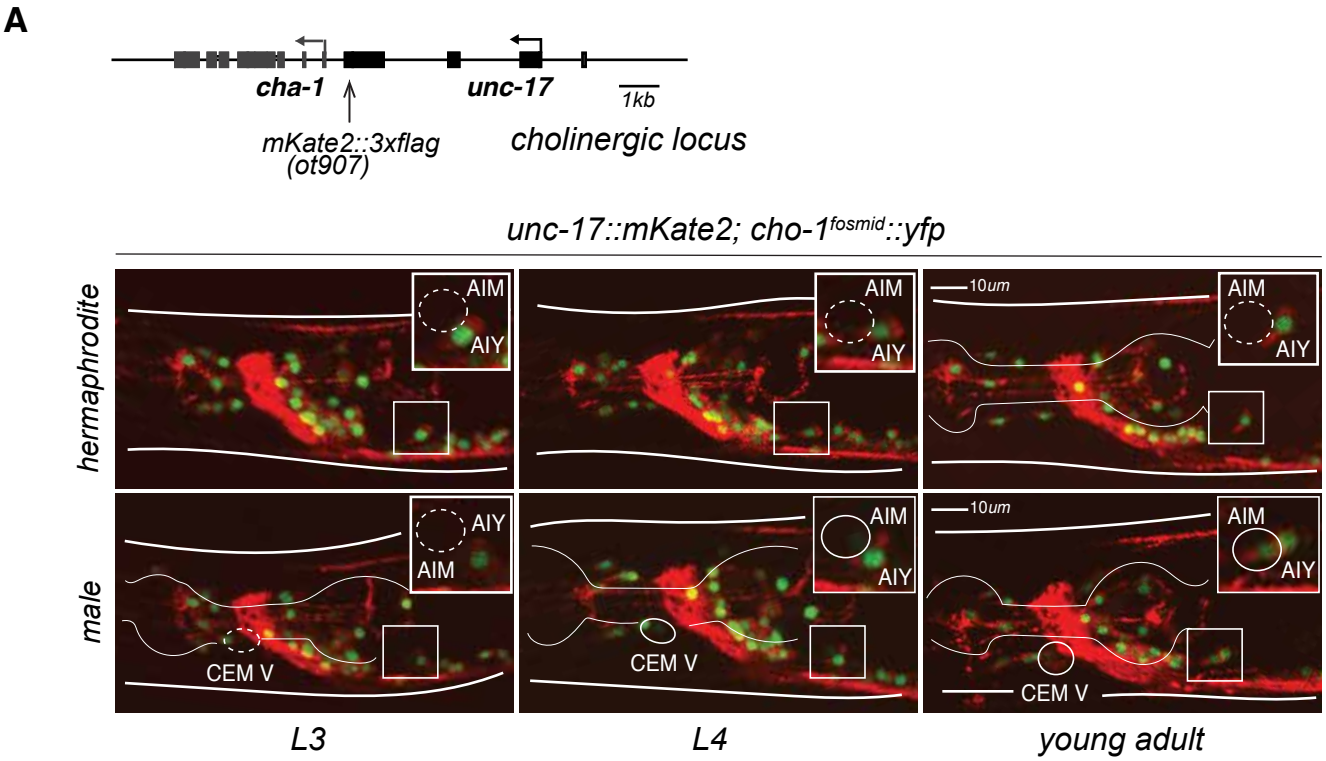

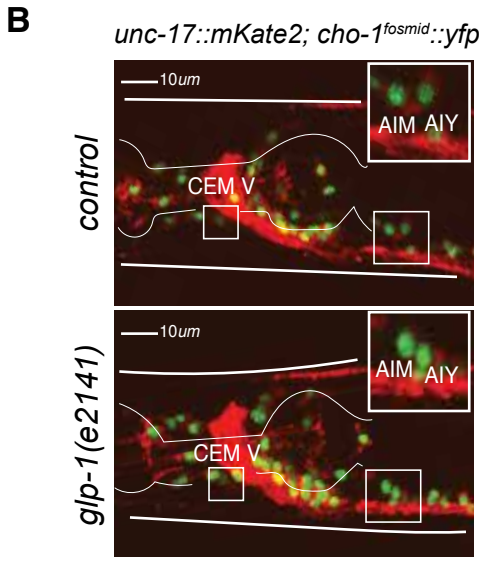

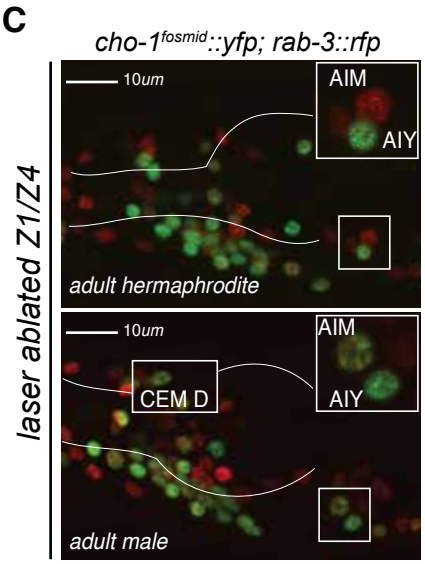

Supplementary Figure 2

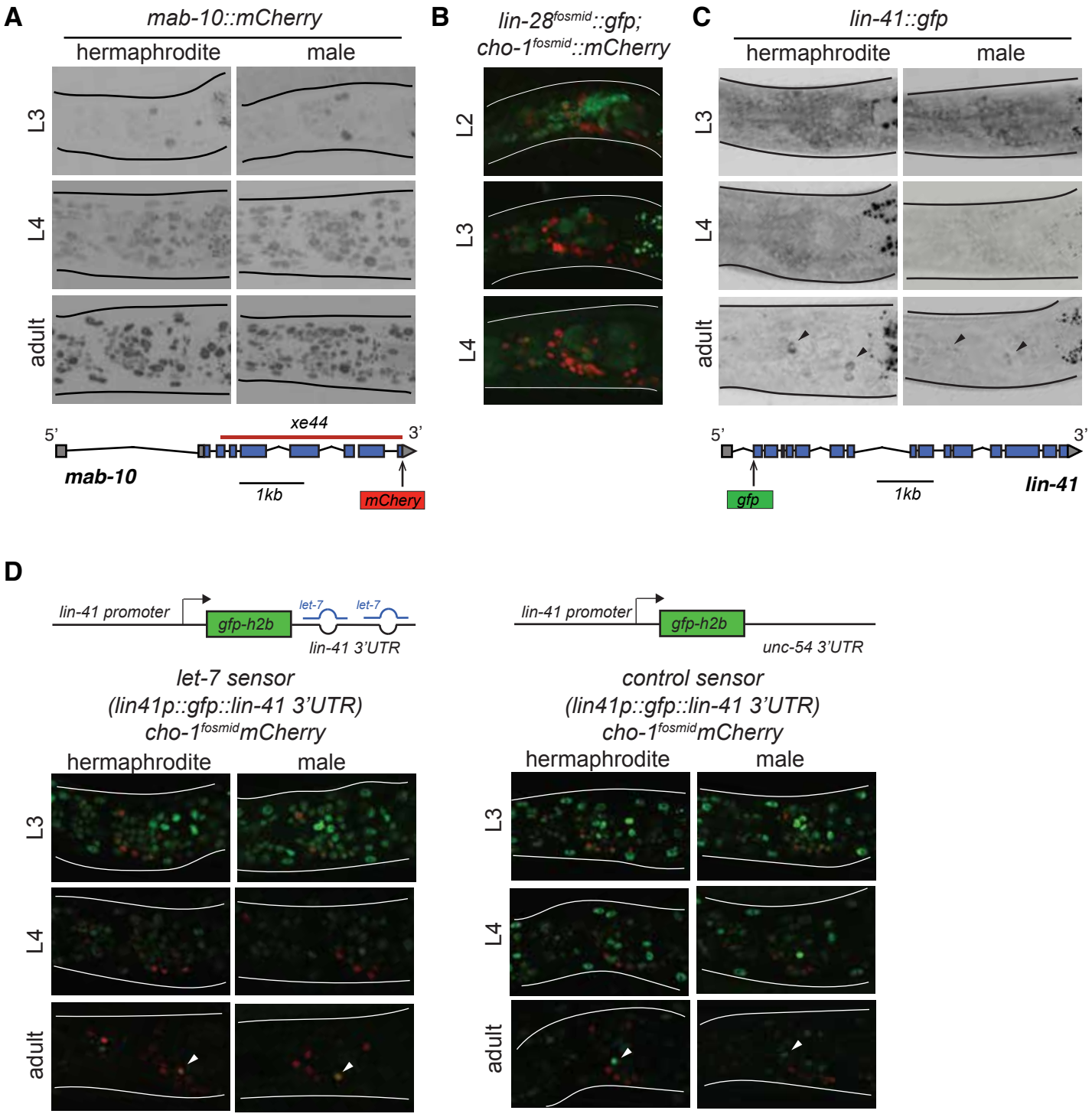

Supplementary Figure 3

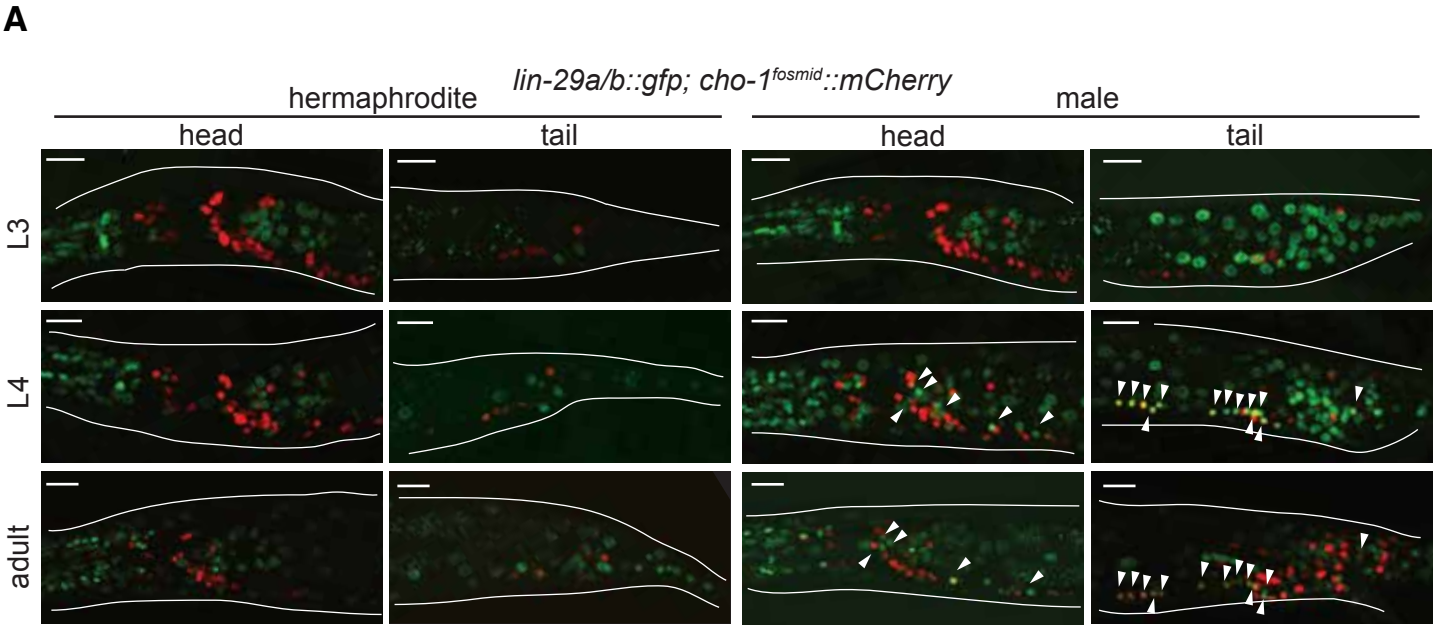

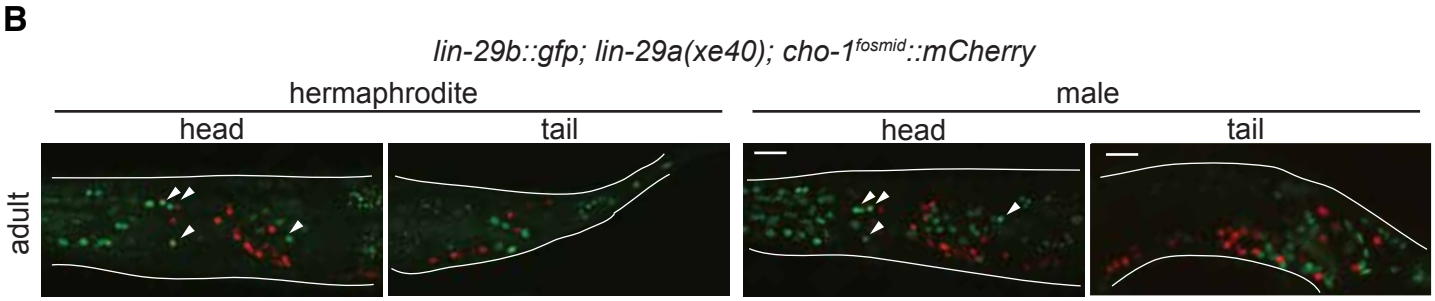

Supplementary Figure 4

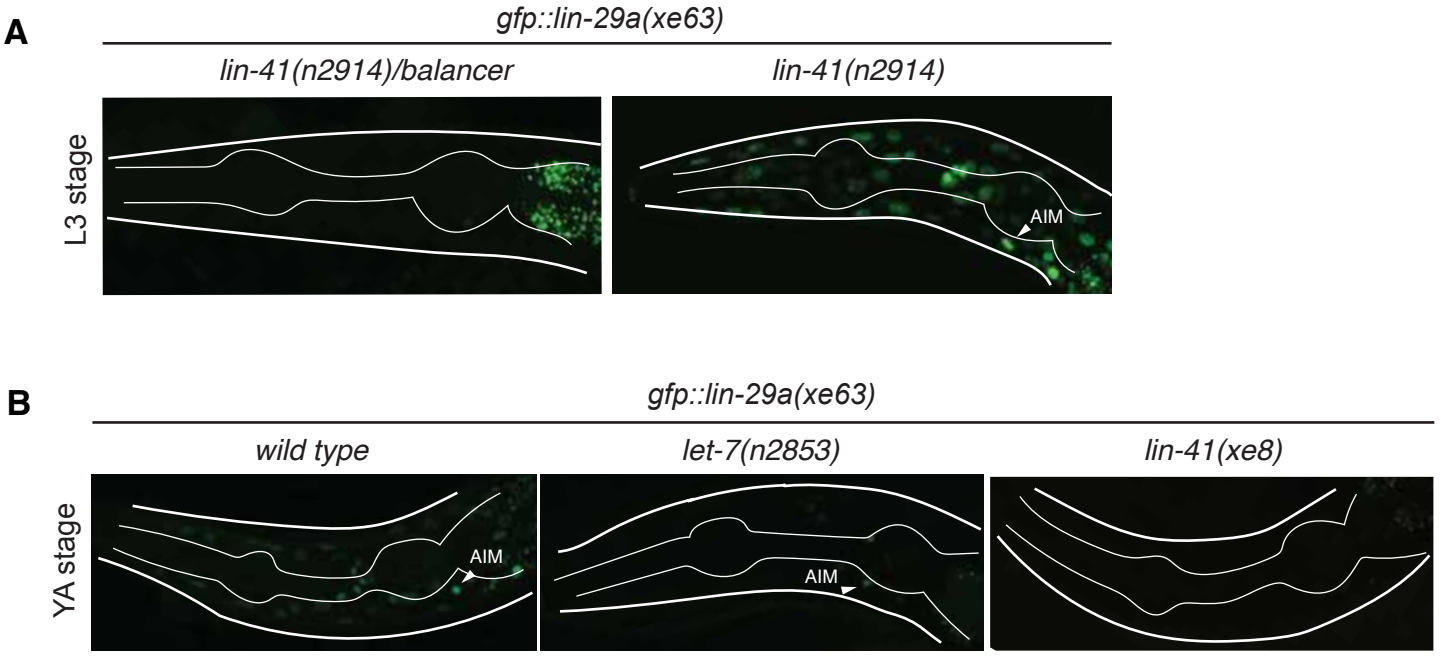

Supplementary Figure 5

A

B

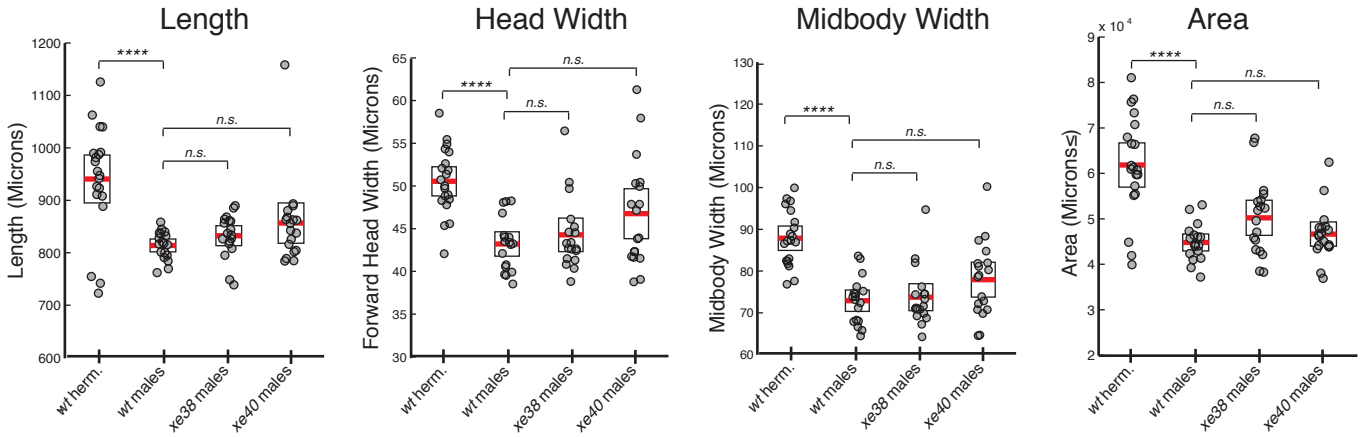

Supplementary Table 1: List of sexually dimorphic *lin-29A* independent locomotory features.

Sexually dimorphic features not affected by *lin-29A* absence	Type
Absolute forward tail bend (degrees)	*posture*
Track length(microns)	*path*
Eccentricity (no units)	*path*
Bend count (counts)	*motion*
Coils Frequency (Hz)	*motion*
Coil Time (seconds)	*posture*
Absolute tail to head orientation (degrees)	*posture*
Absolute eigen projection 1	*posture*
Absolute eigen projection 2	*posture*
Absolute eigen projection 4	*posture*
Forward head-tip speed (microns/seconds)	*motion*
Forward head speed (microns/seconds)	*motion*
Forward tail speed (microns/seconds)	*motion*
Absolute head tip motion direction (degrees/seconds)	*motion*
Absolute head motion direction (degrees/seconds)	*motion*
Absolute tail motion direction (degrees/seconds)	*motion*
Absolute tail-tip motion direction (degrees/seconds)	*motion*
Absolute foraging speed (degrees/seconds)	*motion*
Head crawling frequency (Hz)	*motion*
Midbody crawling frequency (Hz)	*motion*
Tail crawling frequency (Hz)	*motion*
Omega turns frequency (Hz)	*motion*
Worm dwelling (seconds)	*path*

Supplementary Table 2: Strains used in this study

Strain name	Genotype	DNA on array
DR466	*him-5(e1490)*	
MT1524	*lin-28(n719)*	
MT7897	*lin-41(n2914)/unc-29(e1072); lin-11(n1281)*	
MT7626	*let-7(n2853)*	
HW1814	*lin-41(xe8)/(bch-28)*	
VT132	*lin-29(n333)/mnC1; sqt-1(sc13)*	
CB4037	*glp-1(e2141)*	
HW1672	*lin-29(xe37)*	
HW1693	*lin-29(xe38)*	
HW1695	*lin-29(xe40)*	
HW1698	*mab-10(xe44)*	
CB2823	*tra-1(e1488)/eDp6*	
MT1859	*unc-86(n846)*	
OH161	*ttx-3(ot22)*	
CB151	*unc-3(e151)*	
CB419	*unc-42(e419)*	
OH15422	*ceh-14(ot900)* [E.A. Bayer and O.H., unpubl.]	
OH15568	*unc-17(ot907[unc-17::mKate2::3xflag])*	
DG3913	*lin-41(tn1541[lin-41::gfp])*	
HW1822	*lin-29(xe61[lin-29a/b::gfp::3xflag])*	
HW1835	*lin-29(xe63 [gfp::3xflag::lin-29a])*	
HW1883	*lin-29(xe65 [lin-29b::gfp::3xflag; lin-29(xe40)])*	
HW2047	*mab-10(xe75[mab-10::3xflag::mCherry])*	
OH15732	*mab-3(ot931[mab-3::3xflag::gfp])*	
OH15733	*dmd-3(ot932[dmd-3::3xflag::gfp])*	
OH10689	*otIs355*	*rab-3::nls::tag_rfp*
OH12543	*otIs534*	*cho-1 fosmid::sl2::yfp::h2b*
OH12655	*otIs544*	*cho-1 fosmid::sl2::mCherry::h2b*
OH13083	*otIs576*	*unc-17 fosmid::gfp*
OH11124	*otIs388*	*eat-4 fosmid::sl2::yfp::h2b*
OH12496	*otIs518*	*eat-4 fosmid::sl2::mCherry::h2b*
OP535	*wtIs535*	*lin-28 fosmid::gfp*
HW2172	*xeSi182*	*plin-41::gfp(pest)::h2b::lin-41 3'UTR*
HW2173	*xeSi202*	*plin-41::gfp(pest)::h2b::unc-54 3'UTR*
UR219	*fsIs5*	*srj-54p::yfp*
UL2497	*Ex(dmd-5p::gfp)*	*dmd-5p::gfp (pUL#JS9B3 plasmid)*
FK181	*ksIs2*	*daf-7p::gfp*
EB2509	*dzIs75 II*	*kal-1p::gfp*
OH15741	*lin-29(xe38) + otEx7316*	*eat-4p::lin-29a*
OH15742	*lin-29(xe38) + otEx7317*	*eat-4p::lin-29a*
OH15743	*lin-29(xe40) + otEx7318*	*eat-4p::lin-29a*
OH15744	*lin-29(xe40) + otEx7319*	*eat-4p::lin-29a*
OH15745	*lin-29(xe38) + otEx7320*	*unc-17p::lin-29a*
OH15746	*lin-29(xe61) + otEx7321*	*rab-3p::fem-3::mCherry*
OH15748	*mab-3(ot931) + otEx7322*	*rab-3p::fem-3::mCherry*
OH15749	*dmd-3(ot921) + otEx7323*	*rab-3p::fem-3::mCherry*